

Anonymous Referee #1

This study investigated patterns and characteristics of atmospheric new-particle formation events in Beijing. The authors categorized these observed events into three classes based on the number size distributions of the newly-formed particles. Further, by combining the size distribution with the speciation of measured or modelled gas and particle-phase pollutants, the authors discussed the contribution of organic and inorganic compounds to particle growth during different type of events.

The manuscript focus on the topic of new-particle formation in the urban atmosphere, trying to address critical questions that whether or not the newly-formed particles can grow to the CCN size, and what conditions/species control the grow process. The scope of the manuscript is thus suitable for ACP, and the data the authors presented are ample and interesting. However, the interpretation of some key results is questionable and leads to unrigorous conclusions. Major revisions and improvements are needed before this manuscript can be considered for publication as an ACP paper.

Response: The authors thank the reviewer's comments and try our best to respond and revise our manuscript accordingly.

Major comments:

1) The authors defined three classes. "Class I was characterized by no apparent particle growth" makes sense, this class might indicate either a lack of supersaturated condensable vapors so that particles don't grow, or a too high condensation sink so that small particles don't survive. But is there a better way to classify the rest events? Particles are larger than 50 (or 75) nm doesn't necessarily mean they are good CCNs; and there are so many factors (chemical, physical or meteorological) that can determine whether or not the particles grow over 50 (or 75) nm. Classifying the events just based on the "cut-off" size doesn't really help modelers or lab experimentalists to understand the real atmosphere. Please justify the classification or improve it.

Response: When the size of atmospheric particles is smaller than 60 nm (Dusek et al., 2006), the CCN activation of aerosol particles at normal ambient super-saturation has been reported to be determined solely by particle size. In addition to particle size, various factors such as chemical composition, particle mixing states, and meteorological conditions may also largely affect CCN activation of aerosols with D_{pg} beyond 70 nm (Ma et al., 2016; Rose et al., 2017; Lee et al., 2019). Although new particles in Class III can grow to the CCN size, the CCN activation of grown new particles has been reported to vary case by case (Wiedensohler et al., 2009; Yue et al., 2011; Li et al., 2015; Ma et al., 2016). This has been added in the revision (Page 8, Lines 23-27).

As presented in the origin manuscript, currently in Page 2, lines 15-21 of the revision, “Nevertheless, reported observations have also shown that newly formed particles with diameters less than 40–50 nm can be activated as CCN only under high supersaturation (SS), such as >0.6% (Li et al., 2015; Ma et al., 2016). When newly formed particles grow with the geometric median diameter to larger than 70 nm, they significantly contribute to the CCN population at $SS \leq 0.2\%$ (Wiedensohler et al., 2009; Yue et al., 2011; Li et al., 2015; Ma et al., 2016; Zhu et al., 2019). In addition, field observations have also shown that in most NPF events, the maximum geometric median diameter (D_{pgmax}) of newly grown particles is less than 40–50 nm before new particle signals drop to a negligible level (Zhu et al., 2014, Liu et al., 2014; Man et al., 2015; Zhu et al., 2017; Yu et al., 2019).” It is clear that the growth of newly formed particles encountered a ceiling in size less than 40-50 nm during most of NPF events. This was also true in Scenario 1 of Class II in Beijing. The ceiling prevented newly formed particles from growing to the CCN size in Scenario 1 (This has been added in Page 8, lines 12-13). What causes the ceiling in size less than 40-50 nm and what causes newly formed particles growing over the ceiling are crucially important for modelers or lab experimentalists to explore the true contribution of NPF to the population of CCN.

In fact, 50 nm has been widely used a threshold to judge grown new particles as CCN in high supersaturation in review literature (Kerminen et al., 2018). For the threshold of 70 nm, we added “Similar definitions are applied for the SP of grown new particles with D_{pg} reaching over 70 nm, in which grown new particles can be activated as CCN with highly variable activation efficiencies.” Page 6, lines 2-3 in the revision.

2) From the surface plot of these NPF events (e.g. Fig 2a, e; Fig 3a, e; Fig 4a), I don't see any significant band of pre-existing particles. Were these events all observed in very clean days? Or is it because the linear color scale veil the background particles? Please do change to the log color scales.

Response: Thanks for your suggestion. We have changed the liner color scale to the log color scale (see the revised manuscript), and the pre-existing particles are more obvious in the revised figures.

3) The author stated that many growth events lasted for over 10 hrs or even a whole day. Was there any primary emission mixing with the newly-formed particles, e.g. from vehicles, restaurants or factories? Is it true that there was only condensational growth without mixing during the whole period? Please discuss this and also show O:C from the AMS measurement to verify the statement.

Response: The questions reflect the common challenge when a SCANNING particle sizer

operating in LOW time resolution in MINUTES is used for sampling and studying NPF events. However, it is not an issue when a PARALLELING particle sizer operating in high time resolution in ONE SECOND is used for the same target study.

We used a high-time resolution PARALLELING particle sizer, i.e., FMPS, to measure the particle number size distribution (PNSD) in 1 s time resolution. The high time resolution of FMPS can allow clearly identify the signals of newly formed particles from preexisting ambient particles, e.g., freshly emitted particles from combustion, as well as the mixing process of the different types of particles (Liu et al., 2014; Man et al., 2015; Zhu et al., 2017, 2019).

According to our previous studies (e.g. Zhu et al., 2017, ACP) and the review paper by Tuan et al. (2015), the PNSD of traffic emissions are characterized by two peaks, i.e., about 16 nm and 30 nm, and intermittently lasts a few seconds or minutes (Figure R1). Figure R2 (added in new supporting information) shows the fresh industrial emissions associated with SO₂ and/or the cooking emissions associated with increased COA at 18:00-20:00. It is clear that the dominant modes of particles from traffic emissions, industrial emissions and cooking emissions occurred at ~20 nm, ~30 nm and ~40 nm, respectively, and the domain mode size were quietly stable in the study period. Their contributions were important during non-NPF periods, which were not the focus of this study. On the roof sampling site, their contributions to the observed particle concentrations during the initial few hours of NPF were generally negligible in presence of wind speeds of 4-6 m s⁻¹, except a few occasional spikes lasting in minutes. These spikes were excluded in calculating NMINP. In the revision, we add “Note that a few spikes of several minutes were occasionally observed and were excluded to calculate NMINP because they may reflect primary particles from localized sources (Liu et al., 2014; Zhu et al., 2017).”. The same is true in calculating the growth rate of particles, shrinkage rate and D_{pgmax}. Additionally, their influences can also be ignored in studying the growth of newly formed particles when the particles grew over 50 nm.

During the NPF events (e.g. Figure R3), COA occasionally influences the new particles signal, and the growth of new particles was consistent with the increase in MO-OOA and LO-OOA. Therefore, we argued that the growth of new particles depends largely on the condensational growth.

We prefer to add the argument in Supporting Information since the challenge is not immediately related to the samplings and associated analyses presented in the text.

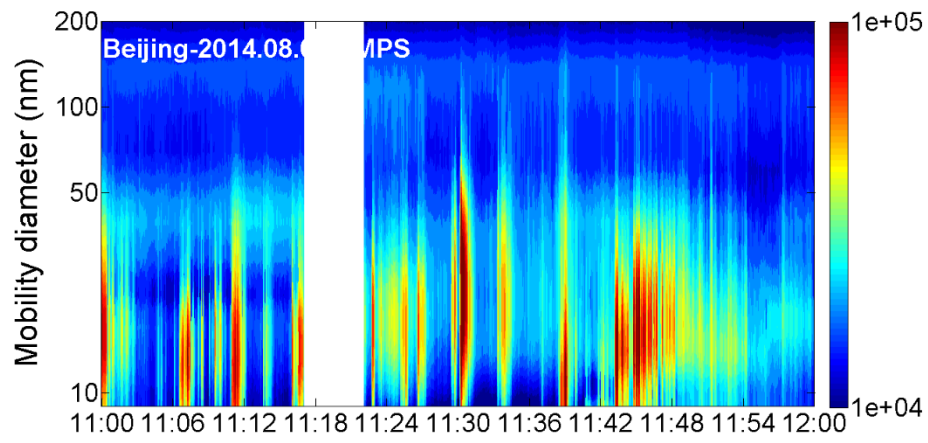


Figure R1 Contour plot of particle number concentrations at the roadside site with spikes from traffic emissions.

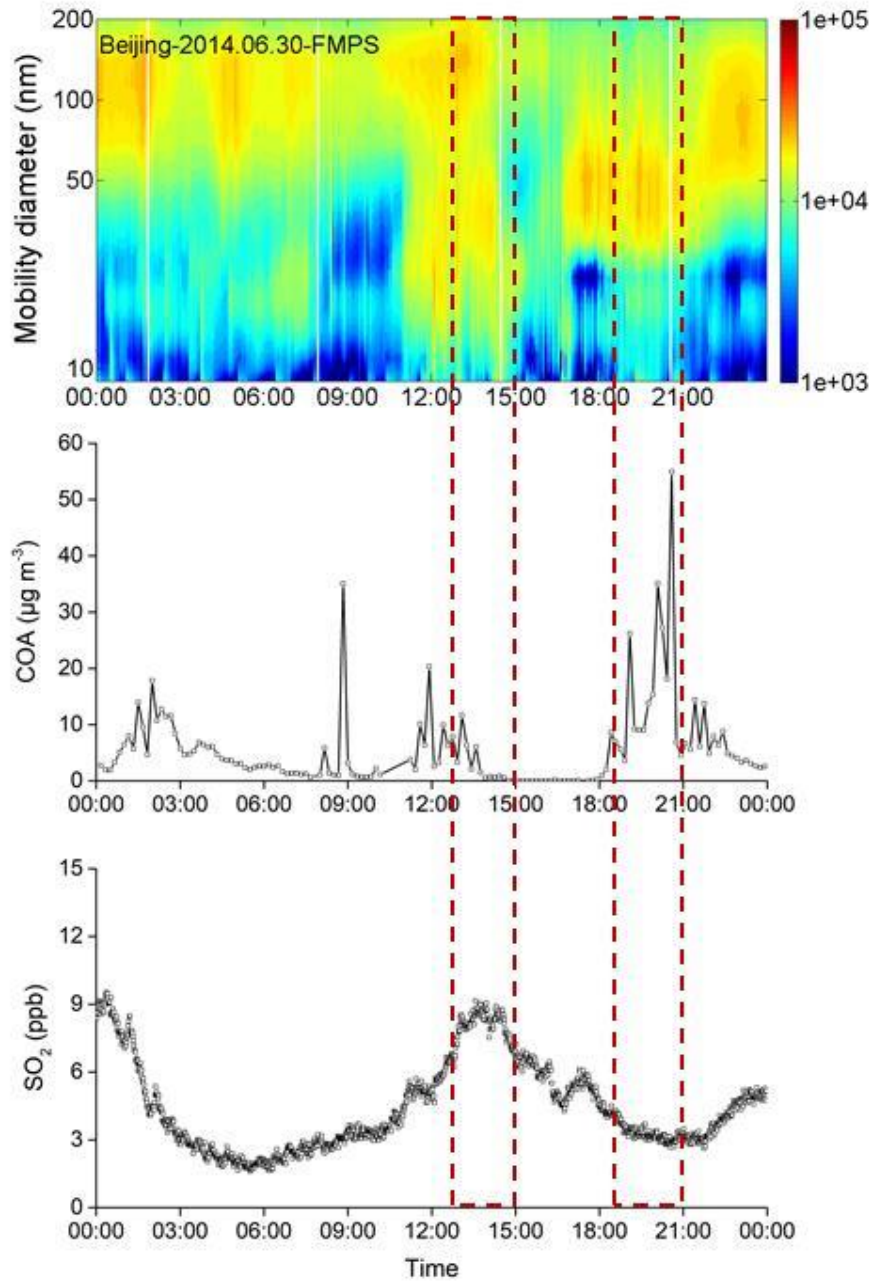


Figure R2 Fresh industrial emissions associated with high SO_2 (12:30-15:00) and cooking emissions with increased cooking OA (COA, 18:20-21:00).

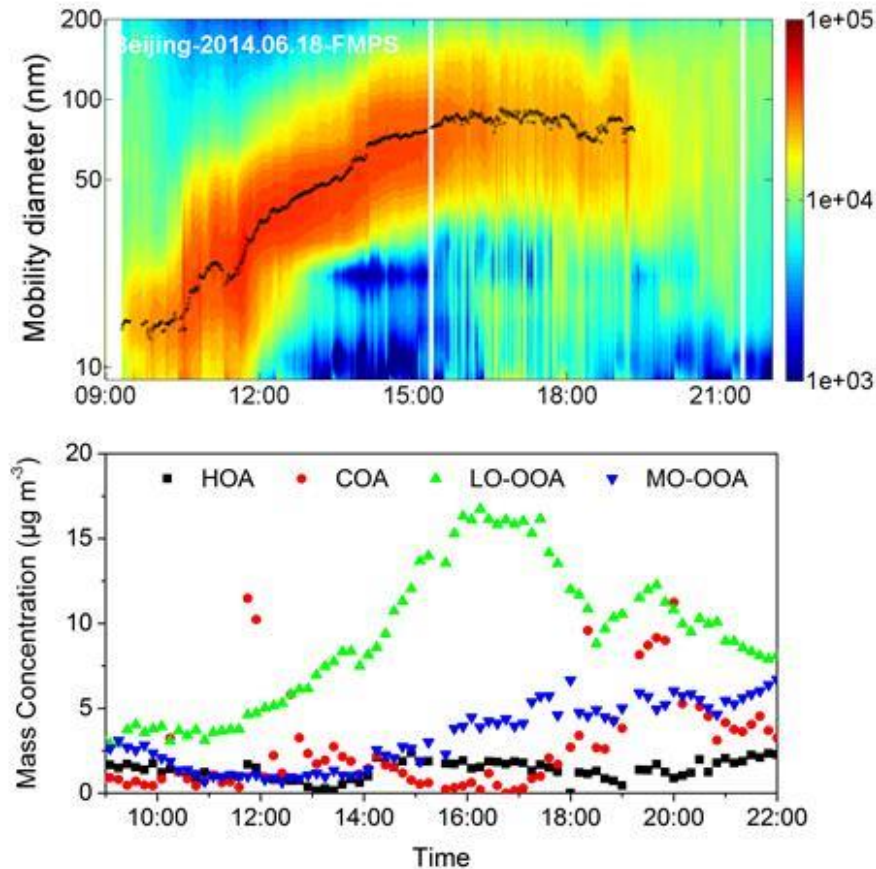


Figure R3 NPF event and variation in hydrocarbon-like OA (HOA), cooking OA (COA), less oxidized oxygenated OA (LO-OOA) and more oxidized oxygenated OA (MO-OOA) on 18 June 2014.

4) *About the AMS measurements, the sampling site is 8 km away from Peking University, how long does it take for an air parcel transport from one site to the other? Roughly one hour maybe? How well does the AMS result represent the particle composition at Peking University? I think this question need to be better addressed in order to discuss the spatial heterogeneity.*

Response: In the revision, page 4, lines 15-21, we add “During NPF events at wind speeds of 4–6 m s^{-1} , a half-hour delay may occur for air parcels sweeping from one site with the FMPS deployed to another site with the AMS deployed. For NPF events with durations over several hours, the events were expected to occur regionally (Kerminen et al., 2018; Chu et al., 2019). Thus, it is reasonable to interpret the cumulative growth of newly formed particles within several hours, measured by the FMPS, by using the net simultaneous change in concentrations of chemical species, measured by the AMS. Additionally, He et al. (2001) reported that the chemical composition of $\text{PM}_{2.5}$ was reasonably homogeneous in the two sampling site zones.”

5) AMS measured the bulk PM_{1.0}, how well does the chemical composition in PM_{1.0} represent the species drive the sub-100 nm particle growth? Were there any aerodynamic diameters measured by AMS at the same time? Discuss more about the uncertainty here.

Response: In the revision, page 4, lines 9-13, we add “The chemical composition of PM_{1.0} measured by AMS has been widely used to interpret NPF events in the literature (Wiedensohler et al., 2009; Zhang et al., 2014; Man et al., 2015; Du et al., 2017; Rodelas et al., 2019; Kanawade et al., 2020) and was also used in this study. Low loadings of particulate chemical species in nanometer size ranges do not facilitate accurate measurement of their concentrations therein. However, the chemical composition of nanometer particles may differ from those of PM_{1.0} (Ehn et al., 2014; Wu et al., 2016).”

In the revision, page 10, lines 13- 24, we add “As mentioned above, the growth of newly formed particles is mainly attributed to sulfuric acid, ammonium nitrate, and secondary organic compounds (Wiedensohler et al., 2009; Riipinen et al., 2011; Zhang et al., 2012; Ehn et al., 2014; Man et al., 2015; Wang et al., 2015; Burkart et al., 2017; Lee et al., 2019; Wang et al., 2020). We therefore explore their respective contributions as follows. First, we calculated the contribution of sulfuric acid to the growth based on the observed mixing ratio of SO₂ and Equations 2–4. Second, we examined whether NH₄NO₃ freshly formed in PM_{1.0} or PM_{2.5} during the particle growth period. In case of no NH₄NO₃ formation, its contribution would not be expected. This is because an even higher product of HNO_{3(gas)}*NH_{3(gas)} is required to overcome the kelvin effect and form NH₄NO₃ in nucleation mode and Aitken mode particles. Thus, the growth unexplained by sulfuric acid should be mainly contributed by SOA. Third, in case of NH₄NO₃ formation, we compared the net increase in NH₄NO₃ with that in SOA. It is noteworthy that this approach is limited by the uncertainty in explaining the growth because the ratios of increased NH₄NO₃ over increased SOA in PM_{1.0} or PM_{2.5} may not be the same as the ratios in nucleation mode and Aitken mode particles. In this case, the required mass of NH₄NO₃ or SOA to the growth was also estimated and compared with their respective net increases to facilitate the analysis.”

6) Page 4, line 20, Equation 4, I don't find the exact same equation in the references the authors cited here. Using averaged particle number concentration over the whole growth period can bring in large uncertainties. Newly-formed particle is prone to coagulation loss; this means particle number concentration at D_{pg1} will be much higher than that at D_{pg2}, and the Mass required

will be overestimated. Please justify the equation, or calculate the particle mass concentration for each FMPS scan and also take the coagulation into account.

Response: Agree. The part has been revised as “The amount of chemical species required to grow new particles from D_{pg1} to D_{pg2} ($Mass_{required}$) is approximately estimated as follows:

$$Mass_{required} = 4/3\pi [(D_{pg2}/2)^3 - (D_{pg1}/2)^3] * N * \rho \quad (5)$$

ρ is the density, which is assumed as $1.5 \mu\text{g m}^{-3}$ for OOA (or SOA) and $1.7 \mu\text{g m}^{-3}$ for NH_4NO_3 , respectively. Considering that the particle number concentration may decrease because of the dry deposition, diffusion and dilution effects, and particle coagulation, N represents the integral value of new particle number concentrations with the geometric median diameter of new particles from $D_{pg2-3\sigma}$ to $D_{pg2+3\sigma}$. The approximate value may overestimate the required amount because particle–particle coagulation has not been deducted.”

However, inclusion of the particle-particle coagulation needs the approximation on the size of particles coagulated from two particles. The approximation would introduce additional uncertainty. We hope that the reviewer can agree on this point.

7) Was there a special reason to sum up O_3 and NO_2 instead of discussing them separately? NO_2 is not always associated with O_3 , it could come from primary emission such as vehicle exhaust.

Response: In China, our previous study showed that the primary on-road vehicular NO_2/NO_x ratio was less than 2%, and NO was the main exhaust gas (Yao et al., 2005). Heavy duty vehicles are allowed to enter urban areas in Beijing only after 20:00 but not in daytime. Considering the NO -titration of O_3 ($\text{O}_3 + \text{NO} \rightarrow \text{NO}_2 + \text{O}_2$), we use the sum of O_3 and NO_2 to represent the oxidizing capacity.

8) The authors briefly mentioned seasonal variation, but didn't dive into the details in, for example, wintertime events. A recent study (Wang et al., 2020, Nature 581 (7807), 184-189) show that NH_4NO_3 could help the newly-formed particles grow and survive in winter. So, it's intriguing to know that the authors observed that the newly formed particles didn't grow during wintertime events, but it would be more important to understand why they didn't. Was it because of a lack of supersaturated condensable vapors, or a too high condensation sink?

Response: Wang et al. (2020) performed the experiments in the CLOUD chamber with scrupulous cleanliness and minimal contamination, and found NH_4NO_3 can drive the newly-formed particles grow to the larger sizes. The reference has been cited in the revision. However, the new finding

needs more field measurements to confirm. In our previous study (Yu et al., 2016), NH_4NO_3 can be formed through artifact reactions when ambient pressure was reduced largely in sampling.

Lack of apparent particle growth during NPF events in December was observed simultaneously at two neighbor sites using two identic FMPS, i.e., a roof site and a roadside site (Zhu et al., 2017), allows us having a strong confidence on the observations. Lack of apparent particle growth was also simultaneously observed during parts of NPF events in April at the two sides using the same methods. The repeated results further confirm the finding. Unfortunately, we had no simultaneous gaseous HNO_3 and NH_3 together with their particulate partners to confirm this. Thus, we cannot speculate more on this issue.

In the chamber study reported by Guo et al. (2020, PNAS, 117, 7, 3427-3432), new particles grew rapidly to about 50 nm in a clean chamber with preexisting particles removed, but they grew much slowly in the polluted air, in which the sizes of new particles grew less than 20 nm (Figure 1 in Guo's paper). Based on Guo's study, the lack of growth of new particle during wintertime was partially due to the high condensation sink. The reference has also been cited in the revision.

9) Please discuss more about the model uncertainty, sensitivity test, etc.

Response: In the revision (Page 7, lines 4-10), we have added “During the study period, the model results generally met the benchmark criteria of the above four species (US-EPA, 2007), with correlations between modeled and measured values larger than 0.57 (Table S1). The modeled concentrations of NH_4^+ reasonably agree with the observations with a normalized mean bias (NMB) of 6%. The NMB slightly increased up to 12% for the modeled concentrations of SO_4^{2-} . The modeled values of NO_3^- and SOA were underestimated with NMBs of -29% and -39%, respectively. Underestimation of SOA is a common weakness of the model simulation because a fraction of SOA precursors are not included, and some key formation pathways of SOA may still be missing in current air quality models (Baek et al., 2011; Knote et al., 2014).”

10) The authors used many sentences describing the particle growth/shrinkage processes vs time, e.g. “However, the shrinkage occurred as early as 15:20-17:20 on 11 June.”. Yet these sentences contain very limited information. I would suggest the authors go through the whole manuscript and reword these sentences by discussing more deeply about the environmental conditions or the causes of these different types of growth.

Response: The detailed analysis was presented in Section 4.3. In the revision (Page 13, lines 19-22), we added “During this period of shrinkage, the observed mixing ratio of O_x largely decreased from 130 ppb to 80 ppb, and the observed OOA decreased from $16.2 \mu\text{g m}^{-3}$ to $11.4 \mu\text{g m}^{-3}$ ”

m^{-3} (Fig. 4b, c). However, the concentrations of NH_4^+ were almost constant. Repartition of the semivolatile SOA in gas and particle phases was hypothesized to cause the evaporation of semivolatile SOA to the gas phase.” Additionally, we had revised our analysis through the manuscript.

Minor comments:

1) Page 1, line 17: “11/27” (and hereinafter) should be something like “11 out of 27”.

Response: Corrected.

2) Page 1, line 22: “... in the remaining NPF events”, please add the number here.

Response: Corrected.

3) Page 2, line 26: “survival probability ratios”, “survival probability” would be better.

Response: Corrected.

4) Page 3, line 9: should the coefficient be size-dependent?

Response: We follow an empirical correction procedure for size distribution data reported by FMPS proposed by we Zimmerman (2015). The coefficient was size in-dependent.

5) Page 3, line 13: “During the other observational periods...”, please specify the date.

Response: Corrected.

6) Page 6, line 8: “to a negligible level; in Scenario 2”, the semicolon should be period.

Response: Corrected.

7) Page 6, line 10: “... may not represent two NPF events occurring in one day.”, why? They look very much like two events.

Response: The sentence has been removed in the revision to avoid confusion.

8) Page 6, line 14: “... associated with wind direction changes in the late afternoon or nighttime.”, please specify the wind directions, and discuss if the sources of pollutants changed.

Response: The sentence has been removed in the text, but the wind speeds and wind directions has been added in the supporting information.

9) Page 7, line 14: “... from 9-22 nm to 23-69 nm...”, please reword it.

Response: Done.

10) Page 8, line 29: “uparticulate” should be “particulate”.

Response: Corrected.

11) Page 9, line 19: “... need to confirm this.”, should be “... are needed to confirm this.”

Response: Corrected.

12) Page 9, line 30: “stopped the growth”, should be “stopped growing”.

Response: Corrected.

13) Page 10, line 17: “The observed concentrations of OM and NO_3^- largely oscillated and had no increasing trends after 21:00, although D_{pg} increased from 60 nm to 75 nm in one and half hours.”, explain this.

Response: In the revised manuscript, we used OOA instead of OM. The part has been revised as (also show in Figure R4) “The observed concentrations of OOA (left axis) and NO_3^- (right axis) rapidly increased from 18:00 to 22:20, with the former being approximately four times larger than the latter. The required amount of NH_4NO_3 for particle growth during the period was estimated to be $5.3 \mu\text{g m}^{-3}$, while the net increase in NH_4NO_3 was $1.6 \mu\text{g m}^{-3}$. SOA may dominate the growth of new particles.”

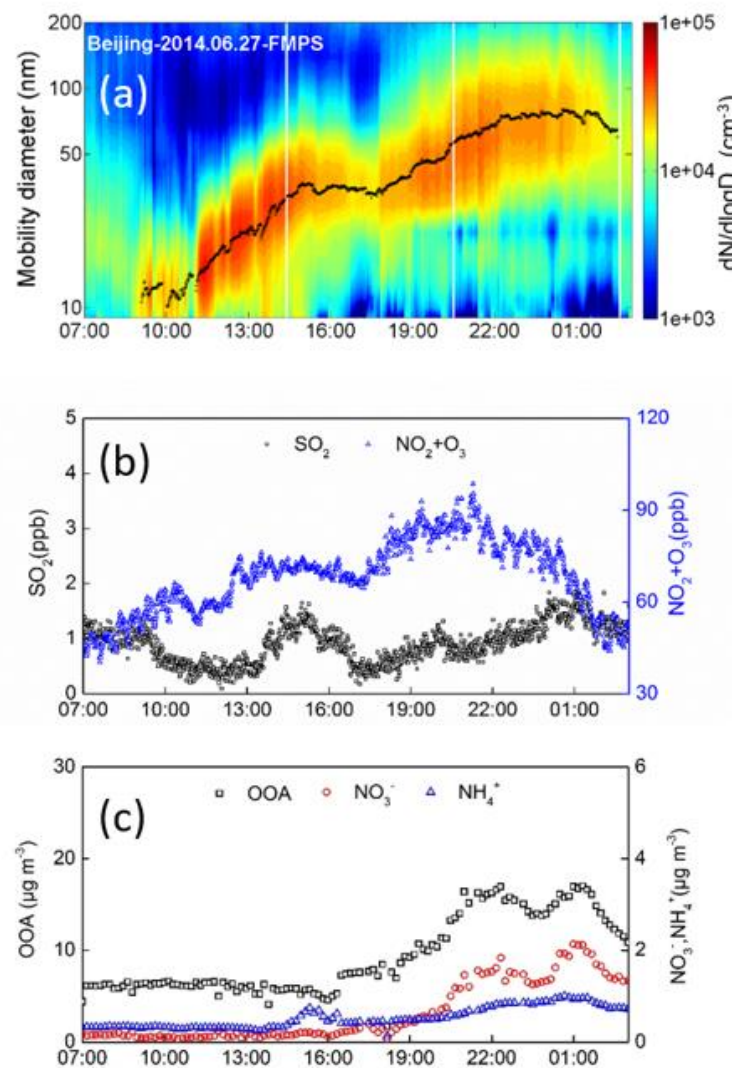


Figure R4 NPF event that occurred on 27 June 2014 ((a) contour plot of the particle number concentration; (b) time series of the observed mixing ratios of SO_2 , NO_2+O_3 (c) time series of observed OOA, NO_3^- and NH_4^+ in $\text{PM}_{1.0}$).

14) Page 12, line 5: “The slope further suggests that an increase of 10 ppb in O_x likely causes an increase of 5 nm in D_{pgmax} .”, I would suggest removing it.

Response: Delete.

15) Page 12, line 23: “When the estimated CS were compared, the averaged value was $1.8\pm 2.0\times 10^{-2} \text{ s}^{-1}$, $2.1\pm 1.5\times 10^{-2} \text{ s}^{-1}$ and $2.0\pm 1.2\times 10^{-2} \text{ s}^{-1}$. . .”, the deviations are too large to provide detailed information, I would suggest removing it.

Response: Delete.

Reference:

- Baek J., Hu Y.T., Odman M.T., Russell A.G.: Modeling secondary organic aerosol in CMAQ using multigenerational oxidation of semi-volatile organic compounds, *J. Geophys. Res.*, 116, D22204, doi: 10.1029/2011JD015911, 2011.
- Burkart, J., Hodshire, A. L., Mungall, E. L., Pierce, J. R., Collins, D.B., Ladino, L. A., Lee, A. K., Irish, V., Wentzell, J. J., Liggio, J., and Papakyriakou, T.: Organic condensation and particle growth to CCN sizes in the summertime marine Arctic is driven by materials more semivolatile than at continental sites, *Geophys. Res. Lett.*, 44, 10725–10734, doi: 10.1002/2017GL075671, 2017.
- Chu, B., Kerminen, V., Bianchi, F., Yan, C., Petäjä, T., and Kulmala, M.: Atmospheric new particle formation in China, *Atmos. Chem. Phys.*, 19, 115-138, doi: 10.5194/acp-19-115-2019, 2019.
- Du, W., Zhao, J., Wang, Y., Zhang, Y., Wang, Q., Xu, W., Chen, C., Han, T., Zhang, F., Li, Z., Fu, P., Li, J., Wang, Z., and Sun, Y.: Simultaneous measurements of particle number size distributions at ground level and 260 m on a meteorological tower in urban Beijing, China, *Atmos. Chem. Phys.*, 17, 6797–6811, <https://doi.org/10.5194/acp-17-6797-2017>, 2017.
- Dusek, U., Frank, G. P., Hildebrandt, L., Curtius, J., Schneider, J., Walter, S., Chand, D., Drewnick, F., Hings, S., Jung, D., Borrmann, S., Andreae, M.O.: Size Matters More Than Chemistry for Cloud-Nucleating Ability of Aerosol Particles. *Science*, 312, 1375-1378, 2006.
- Ehn, M., Thornton, J.A., Kleist, E., Sipilä, M., Junninen, H., Pullinen, I., Springer, M., Rubach, F., Tillmann, R., Lee, B., Lopez-Hilfiker, F., Andres, S., Acir, I., Rissanen, M., Jokinen, T., Schobesberger, S., Kangasluoma, J., Kontkanen, J., Nieminen, T., Kurtén, T., Nielsen, L.B., Jørgensen, S., Kjaergaard, H.G., Canagaratna, M., Maso, M.D., Berndt, T., Petäjä, T., Wahner, A., Kerminen, V., Kulmala, M., Worsnop, D.R., Wildt, J., and Mentel, T.F.: A large source of low-volatility secondary organic aerosol, *Nature*, 506, 476-479, doi: 10.1038/nature13032, 2014.
- Guo, S., Hu, M., Peng, J., Wu, Z., Zamora, M. L., Shang, D., Du, Z., Zheng, J., Fang, X., Tang, R., Wu, Y., Zeng, L., Shuai, S., Zhang, W., Wang, Y., Ji, Y., Zhang, A., Wang, W., Zhang, F., Zhao, J., Gong, X., Wang, C., Molina, M., Zhang, R.: Remarkable nucleation and growth of ultrafine particles from vehicular exhaust. *P. Natl. Acad. Sci.*, 117(7), 3427-3432, 2020.
- He, K.B., Yang, F.M., Ma, Y.L., Zhang, Q., Yao, X.H., Chan, C.K., Cadle, S., Chan, T., and Mulawa, P.: The characteristics of PM_{2.5} in Beijing, China. *Atmos. Environ.*, 35, 4959-4970, doi: 10.1016/S1352-2310(01)00301-6, 2001.
- Kanawade, V. P., Tripathi, S. N., Chakraborty, A., and Yu, H.: Chemical Characterization of Sub-micron Aerosols during New Particle Formation in an Urban Atmosphere, *Aerosol Air Qual. Res.*, 20(6): 1294-1305, doi: 10.4209/aaqr.2019.04.0196, 2020.
- Kerminen, V., Chen, X., Vakkari, V., Petäjä, T., Kulmala, M., and Bianchi, F.: Atmospheric new particle formation and growth: review of field observations, *Environ. Res. Lett.*, 13, 103003, doi: 10.1088/1748-9326/aadf3c, 2018.
- Knote C., Hodzic A., Jimenez J.L., Volkamer R., Orlando J.J., Baidar S., Brioude J., Fast J., Gentner D.R., Goldstein A.H., Hayes P.L., Knighton W.B., Oetjen H., Setyan A., Stark H., Thalman R., Tyndall G., Washenfelder R., Waxman E. and Zhang Q.: Simulation of semi-explicit mechanisms of SOA formation from glyoxal in aerosol in a 3-D model, *Atmos. Chem. Phys.*, 14, 6213-6239, doi:10.5194/acp-14-6213-2014, 2014.
- Lee, S., Gordon, H., Yu, H., Lehtipalo, K., Haley, R., Li, Y., and Zhang, R.: New Particle Formation in the Atmosphere: From Molecular Clusters to Global Climate, *J. Geophys. Res. Atmos.*, 124, 7098-7146, doi: 10.1029/2018JD029356, 2019.
- Li, J., Yin, Y., Li, P., Li, Z., Li, R., Cribb, M., Dong, Z., Zhang, F., Li, J., Ren, G., Jin, L., and Li,

- Y.: Aircraft measurements of the vertical distribution and activation property of aerosol particles over the Loess Plateau in China, *Atmos. Res.*, 155, 73-86, doi: 10.1016/j.atmosres.2014.12.004, 2015.
- Liu, X.H., Zhu, Y.J., Zheng, M., Gao, H.W., Yao, X.H.: Production and growth of new particles during two cruise campaigns in the marginal seas of China. *Atmos. Chem. Phys.*, 14, 7941-7951, 2014.
- Ma, N., Zhao, C., Tao, J., Wu, Z., Kecorius, S., Wang, Z., Größ, J., Liu, H., Bian, Y., Kuang, Y., Teich, M., Spindler, G., Müller, K., van Pinxteren, D., Herrmann, H., Hu, M., and Wiedensohler, A.: Variation of CCN activity during new particle formation events in the North China Plain. *Atmos. Chem. Phys.*, 16, 8593-8607, 2016.
- Man, H., Zhu, Y., Ji, F., Yao, X., Lau, N. T., Li, Y. J., Lee, B.P., Chan, C.K.: Comparison of daytime and nighttime new particle growth at the HKUST Supersite in Hong Kong, *Environ. Sci & Technol.*, 49 (12), 7170-7178, 2015.
- Rodelas, R.R, Chakraborty, A, Perdrix, E, Tison, E, Riffault, V.: Real-time assessment of wintertime organic aerosol characteristics and sources at a suburban site in northern France. *Atmos. Environ.*, 203, 48-61, 2019.
- Riipinen, I., Pierce, J. R., Yli-Juuti, T., Nieminen, T., Häkkinen, S., Ehn, M., ... Kulmala, M. (2011). Organic condensation: A vital link connecting aerosol formation to cloud condensation nuclei (CCN) concentrations. *Atmos. Chem. Phys.*, 11(8), 3865–3878, doi:10.5194/acp-11-3865-2011.
- Tuan, V., Delgadoaborit, J. M., and Harrison, R. M.: Review: Particle number size distributions from seven major sources and implications for source apportionment studies. *Atmos. Environ.*, 114-132, 2015.
- Wang, Z.B., Hu, M., Pei, X.Y., Zhang, R.Y., Paasonen, P., Zheng, J., Yue, D.L., Wu, Z.J., Boy, M., and Wiedensohler, A.: Connection of organics to atmospheric new particle formation and growth at an urban site of Beijing, *Atmos. Environ.*, 103, 7-17, doi:10.1016/j.atmosenv.2014.11.069, 2015.
- Wang, M., Kong, W., Marten, R., He, X., Chen, D., Pfeifer, J., Heitto, A., Kontkanen, J., Dada, L., Kürten, A., Yli-Juuti, T., Manninen, H., Amanatidis, S., Amorim, A., Baalbaki, R., Baccarini, A., Bell, D., Bertozzi, B., Bräkling, S., Brilke, S., Murillo, U. C., Chiu, R., Chu, B., De Menezes, L-P., Duplissy, J., Finkenzeller, H., Carracedo, L. G., Granzin, M., Guida, R., Hansel, A., Hofbauer, V., Krechmer, J., Lehtipalo, K., Lamkaddam, H., Lampimäki, M., Lee, C.P., Makhmutov, V., Marie, G., Mathot, S., Mauldin, R. L., Mentler, B., Müller, T., Onnela, A., Partoll, E., Petäjä, T., Philippov, M., Pospisilova, V., Ranjithkumar, A., Rissanen, M., Rörup, B., Scholz, W., Shen, J., Simon, M., Sipilä, M., Steiner, G., Stolzenburg, D., Tham, Y. J., Tomé, A., Wagner, A. C., Wang, D. S., Wang, Y., Weber, S.K., Winkler, P. M., Wlasits, P. J., Wu, Y., Xiao, M., Ye, Q., Zauner-Wieczorek, M., Zhou, X., Volkamer, R., Riipinen, I., Dommen, J., Curtius, J., Baltensperger, U., Kulmala, M., Worsnop, D. R., Kirkby, J., Seinfeld, J. H., El-Haddad, I., Flagan, R. C., and Donahue, N. M.: Rapid growth of new atmospheric particles by nitric acid and ammonia condensation, *Nature* 581, 184–189, doi: 10.1038/s41586-020-2270-4, 2020.
- Wiedensohler, A., Cheng, Y.F., Nowak, A., Wehner, B., Achtert, P., Berghof, M., Birmili, W., Wu Z.J., Hu, M., Zhu, T., Takegawa, N., Kita, K., Kondo, Y., Lou, S.R., Hofzumahaus, A., Holland, F., Wahner, A., Gunthe, S.S, Rose, D., Su, H., Pöschl, U.: Rapid aerosol particle growth and increase of cloud condensation nucleus activity by secondary aerosol formation and condensation: A case study for regional air pollution in northeastern china, *J. Geophys. Res.*, 114, D00G08, doi: org/10.1029/2008JD010884, 2009.
- Wu, Z.J., Zheng, J., Shang, D.J., Du, Z.F., Wu, Y.S., Zeng, L.M., Wiedensohler, A., and Hu, M.: Particle hygroscopicity and its link to chemical composition in the urban atmosphere of Beijing, China, during summertime, *Atmos. Chem. Phys.*, 16, 1123-1138, doi: 10.5194/acp-16-1123-2016, 2016.

- Yao, X. H., Lau, N. T., Fang, M., Chan, C. K. The use of tunnel concentration profile data to determine the ratio of NO₂/NO_x directly emitted from vehicles. *Atmos. Chem. Phys. Discussions*, 5 (6), 12723-12740, 2005.
- Yu P., Hu, Q., Li, K., Zhu, Y., Liu, X., Gao, H., Yao, X.H. Characteristics of dimethylammonium and trimethylammonium in atmospheric particles ranging from supermicron to nanometer sizes over eutrophic marginal seas of China and oligotrophic open oceans. *Science of the Total Environment*, 572, DOI: 10.1016/j.scitotenv.2016.07.114, 2016.
- Zhang, R., Khalizov, A., Wang, L., Hu, M., and Xu, W.: Nucleation and Growth of Nanoparticles in the Atmosphere, *Chem. Rev.*, 112, 1957-2011, doi: 10.1021/cr2001756, 2012.
- Zhang, Y. M., Zhang, X. Y., Sun, J. Y., Hu, G. Y., Shen, X. J., Wang, Y. Q., Wang, T. T., Wang, D. Z., and Zhao, Y.: Chemical composition and mass size distribution of PM₁ at an elevated site in central east China, *Atmos. Chem. Phys.*, 14, 12237–12249, doi: 10.5194/acp-14-12237-2014, 2014.
- Zhu, Y., Li, K., Shen, Y., Gao, Y., Liu, X., Yu, Y., Gao, H., and Yao, X.: New particle formation in the marine atmosphere during seven cruise campaigns, *Atmos. Chem. Phys.*, 19, 89-113, 2019.
- Zhu, Y., Yan, C., Zhang, R., Wang, Z., Zheng, M., Gao, H., Gao, Y., and Yao, X.: Simultaneous measurements of new particle formation at 1 s time resolution at a street site and a rooftop site, *Atmos. Chem. Phys.*, 17, 9469-9484, 2017.

Anonymous Referee #2

This study investigated seasonal variations of new particle formation (NPF) events in Beijing by using observations of particle size distributions and chemical compositions of aerosols and numerical model simulations. The authors found no apparent growth of new particles in winter whereas the growth of new particles to CCN size (50 or 75 nm) was often observed in summer. The three patterns of NPF events during the summertime were discussed in terms of secondary aerosol formation, evaporation of semi-volatile species, and spatial heterogeneity of NPF events.

The scope of this manuscript is well suited to ACP, and the data obtained by the authors are valuable and important to understand the mechanisms of NPF events in urban atmospheres. However, the current manuscript needs substantial revisions before the manuscript is considered as a publication of ACP as shown below.

Response: Thanks for the reviewer's comments. We will try our best to respond and revise our manuscript accordingly.

1) Page 1, Line 17:

“11/27” should be revised. For example, “11 new particle formation (NPF) events out of 27 events” may be better. Other parts written similarly in the text should also be revised.

Response: Thanks. All these have been revised accordingly.

2) Page 2, Lines 21-28:

The authors described what they did in this study. However, it is not clear to me which parts of this manuscript are scientifically new. There are many previous studies on NPF in Beijing and other urban areas. The authors should summarize these previous studies and describe what are well understood and what are poorly understood in Introduction. Then, the objectives of this study should be described more clearly.

The sentence at Lines 18-20 (Thus far, which chemicals drive the growth.) is a point poorly understood, but I don't think the understanding on this point was improved by this study.

Response: In the revision (Page 2, line 24 – Page 3, line 9), we added “With distinctive particle growth patterns being widely reported, Beijing is an ideal area for studying the growth of newly formed particles (Wehner et al., 2004; Wu et al., 2007, 2016; Wiedensohler et al., 2009; Yue et al., 2010; Matsui et al., 2011; Wang et al., 2013; Guo et al., 2014, 2020; Du et al., 2017; Zhu et al., 2017; Brean et al., 2019; Chen et al., 2019). For instance, as the first study of NPF events in Beijing, Wehner et al. (2004) reported a small growth rate ($\sim 1 \text{ nm h}^{-1}$) of newly formed particles during 25 days from March 05 to April 18, 2004. Such small growth rates are unlikely to facilitate the growth

of particles to reach CCN sizes prior to removal from ambient air because of the large coagulation loss in Beijing (Kulmala and Kerminen, 2008; Kulmala et al., 2016; Chu et al., 2019; Guo et al., 2020). Similar to this finding, no apparent growth of newly formed particles with the D_{pgmax} of approximately 10 nm always occurred in December 2011 at the same campus in Beijing (Zhu et al., 2017). In contrast, the growth of newly formed particles to CCN size and even larger has also been observed in Beijing (Wu et al., 2007; Wiedensohler et al., 2009; Yue et al., 2010; Wang et al., 2013; Guo et al., 2014; Wu et al., 2016). The patterns of particle growth have not been well characterized. Nevertheless, sulfuric acid and/or organic vapors have been proposed to drive particle growth in different NPF events (Wiedensohler et al., 2009; Yue et al., 2010; Wu et al., 2016). Recently, the formation of NH_4NO_3 has been proposed as a driver of the rapid growth of newly formed particles in field studies and chamber experiments (Zhu et al., 2014; Man et al., 2015; Wang et al., 2020). The role of NH_4NO_3 in the growth of newly formed particles in Beijing remains poorly understood. Matsui et al. (2011) and Chen et al. (2019) simulated NPF and the growth of newly formed particles based on observations, but the modeling results were explained with large uncertainties.”

The sentence at Lines 18-20 of the origin manuscript has been revised as “Thus, it is important to characterize NPF events, based on the D_{pgmax} of grown new particles, and to explore the chemicals driving the growth of newly formed particles with D_{pgmax} greater than 70 nm”. Moreover, we add the logic flow in analyzing which chemicals drive the growth in newly formed particles beyond 70 nm. Please see our response to Question 6.

3) Page 4, Line 3: Equation (2)

Please add descriptions on the uncertainty of this equation.

Response: In the revision (Page 5, lines 8-9), we added “The reported error was within 20% for the calculated concentrations against the observations in Beijing (Lu et al., 2019).”

4) Page 4, Line 11:

The SPR analysis (section 4.5) is not meaningful. It is hard to quantitatively estimate the survival fraction of new particles from this equation because the SPR values can be greater than 100% in many cases (Table 1). I think the authors may be able to calculate the loss rate of new particles during each NPF event from CS.

Response: We agree that it does not make sense to calculate the SP beyond 100% because of highly spatial-heterogeneity of NPF in those particular events. In the revision (page 6, lines 4-6), we added “Note that the observed number concentrations of newly grown particles with a larger size sometimes exceeded those with a smaller size under the condition of spatial heterogeneity of NPF. In these cases, that is, NPF events occurring on June 23, and August 12 and 15, SP was not calculated.”

The calculated SP is still, however, valid for most of NPF events, which were only slightly affected by the spatial heterogeneity. We rewrote the section 4.5 in the revision.

We argue that the calculated loss rate of new particles would underestimate the contribution of new particles to the population of CCN by even more against the calculated SP. Supposed that NPF mainly occurred at the upper boundary layer, residual layer or upper free troposphere, these grown new particles were mixed down and detected at the building roof site. In contrast, primarily emitted particles were mainly derived from sources at the lower boundary layer. When the particles in different sizes measured at the roof site were used to calculate the loss rate of new particles, the calculated values should be treated as the maximum loss. The loss rate of new particles at loft would be smaller than the calculated value, but the grown new particles at loft rather than at the roof level would act a potential source of CCN. The calculated SP from the observations may be also affected by the increasing loadings of particles when grown new particles mixed down. However, the extent should be smaller than the calculated loss.

Ideally, the vertical profiles of particle number size distributions would be the best to estimate the SP. However, it is practically difficult to obtain the data.

5) Page 4, Line 13:

Please clarify why 3 sigma was chosen.

Response: The particle number concentration follows the lognormal distribution. In the function curve, 1 sigma covers 68% area, 2 sigma covers 95% area, and 3 sigma covers 99% area. In this study, we use 3 sigma to represent almost all particles in this mode. In the revision, we add “ 3σ covering 99% of the mode particles”. In fact, 3 sigma is quietly common approach used in various studies.

6) Page 4, Line 20: *Mass_{required}*

The authors compared $Mass_{required}$ with the changes in mass concentrations of organic and nitrate aerosols, but the latter is generally controlled by accumulation mode particles, not nucleation mode particles. The comparison between $Mass_{required}$ (changes in aerosol mass for nucleation or Aitken mode particles) and the changes in mass concentrations of organic and nitrate aerosols (mainly controlled by accumulation mode particles) is therefore not so meaningful (in sections 4.1-4.3).

Response: In the revision (Page 10, lines 13-24), we added the logic flow in data analysis. It reads as “As mentioned above, the growth of newly formed particles is mainly attributed to sulfuric acid, ammonium nitrate, and secondary organic compounds (Wiedensohler et al., 2009; Riipinen et al.,

2011; Zhang et al., 2012; Ehn et al., 2014; Man et al., 2015; Wang et al., 2015; Burkart et al., 2017; Lee et al., 2019; Wang et al., 2020). We therefore explore their respective contributions as follows. First, we calculated the contribution of sulfuric acid to the growth based on the observed mixing ratio of SO₂ and Equations 2–4. Second, we examined whether NH₄NO₃ freshly formed in PM_{1.0} or PM_{2.5} during the particle growth period. In case of no NH₄NO₃ formation, its contribution would not be expected. This is because an even higher product of HNO_{3gas}*NH_{3gas} is required to overcome the kelvin effect and form NH₄NO₃ in nucleation mode and Aitken mode particles. Thus, the growth unexplained by sulfuric acid should be mainly contributed by SOA. Third, in case of NH₄NO₃ formation, we compared the net increase in NH₄NO₃ with that in SOA. It is noteworthy that this approach is limited by the uncertainty in explaining the growth because the ratios of increased NH₄NO₃ over increased SOA in PM_{1.0} or PM_{2.5} may not be the same as the ratios in nucleation mode and Aitken mode particles. In this case, the required mass of NH₄NO₃ or SOA to the growth was also estimated and compared with their respective net increases to facilitate the analysis.”

In absence of accurate concentrations of chemical compounds in nucleation mode and Aitken mode particles, the above-mentioned approach is one of most reasonable ways to study the growth of newly formed particles. It is an urgent task to accurately measured concentrations of chemicals in those smaller nanometer particles. Unfortunately, no such technologies are commercially available in research community so far.

7) Page 5, Lines 1-2:

Please provide some brief descriptions on model setups.

Response: In the revision (Page 6, lines 21-26), we added “The initial and boundary conditions were obtained from the National Center for Environmental Prediction (NCEP) FNL (Final) Operational Global Analysis datasets (<http://rda.ucar.edu/datasets/ds083.2>). The major physics options included the Lin microphysics scheme, RRTM long-wave radiation scheme, Goddard short wave scheme, Monin-Obukhov surface-layer scheme, thermal diffusion land-surface scheme, and YSU land-surface scheme. The WRF hourly output files were processed using the Meteorology-Chemistry Interface Processor (MCIP v4.3).”

8) Pages 5, Lines 8-9:

Please describe on model evaluations more clearly (e.g., the degree of agreement with observations, chemical species evaluated).

Response: In the revision (Page 7, lines 4-11), we added “During the study period, the model results generally met the benchmark criteria of the above four species (US-EPA, 2007), with correlations between modeled and measured values larger than 0.57 (Table S1). The modeled concentrations of

NH₄⁺ reasonably agree with the observations with a normalized mean bias (NMB) of 6%. The NMB slightly increased up to 12% for the modeled concentrations of SO₄²⁻. The modeled values of NO₃⁻ and SOA were underestimated with NMBs of -29% and -39%, respectively. Underestimation of SOA is a common weakness of the model simulation because a fraction of SOA precursors are not included, and some key formation pathways of SOA may still be missing in current air quality models (Baek et al., 2011; Knote et al., 2014). Detailed evaluation results of this study are provided in the Supporting Information.”

9) Page 5, Lines 23-27:

The unit of number concentrations in this paragraph is probably not correct.

Response: Thanks and correct.

10) Page 6, Lines 2-19:

Please clarify why Class II was subclassified to 4 scenarios. What is the purpose of this?

Response: In the revision (Page 8, lines 11-14), we added “ The growth of newly formed particles seemingly encountered a ceiling in Scenario 1, in which new particles grown at the maximum D_{pg} unlikely contributed to CCN at normal SS. The ceiling prevented newly formed particles from growing to the CCN size in Scenario 1. The possibility of new particles to grow to CCN size in Scenarios 2–4 remains unknown.”

In four scenarios of Type II, Scenario 1 showed a clear evidence, i.e., there was a ceiling existing in the growth of new particles below 50 nm. This is important for modeling and lab studies to explore what cause the ceiling. There was no clear evidences in Scenarios 2-4, where newly formed particles can grow to CCN size. Of course, there was also no clear evidence existing the ceiling.

11) Page 8, Line 3: *the contribution of <2%*

Please clarify how the authors estimated this contribution. I think the authors have sulfate data observed by AMS. The data can be shown like OM and nitrate in Figures 2-4.

Response: In the revision (Page 5, lines 15-22), we added the equation to calculate the contribution. Please see the revised part.

We believe that the contribution of sulfuric acid to the growth of newly formed particles was much more accurate than the use of the sulfate data observed by AMS. The reason is same as the reviewer’s comments in 6).

12) Page 8, Line 7: 13 ug m⁻³

Please clarify how the authors estimated this value. Did the authors consider the spread of particle size distributions? (like 3 sigma in equation (3)).

Response: In the revision (Page 6, lines 7-14), we added “The amount of chemical species required to grow new particles from D_{pg1} to D_{pg2} (Mass_{required}) is approximately estimated as follows:

$$\text{Mass}_{\text{required}} = 4/3\pi [(D_{\text{pg2}}/2)^3 - (D_{\text{pg1}}/2)^3] * N * \rho \quad (5)$$

ρ is the density, which is assumed as 1.5 $\mu\text{g m}^{-3}$ for OOA (or SOA) and 1.7 $\mu\text{g m}^{-3}$ for NH₄NO₃, respectively. Considering that the particle number concentration may decrease because of the dry deposition, diffusion and dilution effects, and particle coagulation, N represents the integral value of new particle number concentrations with the geometric median diameter of new particles from D_{pg2-3 σ} to D_{pg2+3 σ} . The approximate value may overestimate the required amount because particle–particle coagulation has not been deducted.”

13) Page 8, Lines 6-8:

As I described above, the comparison between the required mass (13 ug m⁻³) and PM_{1.0} enhancement (15 ug m⁻³) is not so meaningful because the former focuses on nucleation/Aitken mode particles but the latter is usually dominated by accumulation mode particles.

I think what the authors can do here is to calculate mass concentration changes for sulfate, nitrate, ammonium, and SOA and to discuss which changes are the largest during the growth periods of new particles.

Response: In the revision (Page 10, lines 13-24), we added the logic flow in data analysis. Please see our response to comment 6). Using the logic flow, we revised our analysis accordingly through the manuscript. Please see the revision.

14) Page 8, Line 7:

OM can be divided into HOA (POA like) and OOA (SOA like) by using m44 and m57 signals. Only OOA can contribute to the growth of particles.

Response: Agree. In the revised manuscript, we use the OOA data instead of OM to discuss the growth of new particles. Please see the revision.

15) Page 9, Lines 3-4:

I don't agree with this authors' description. The simulated OA and nitrate cannot be used to interpret the data unless the authors evaluate the simulations with observations.

Response: See our responses to comment 8).

16) Page 10, Line 16 Delete “(ON)”.

Response: Corrected.

17) Page 10, Line 28: OM can be divided to HOA and OOA as I described above.

Response: We will change OM to OOA in the main text and figures.

18) Page 11, Lines 5-6: “Repartition of the...” This part should be removed because no data can support this sentence.

Response: In the revision (Page 13, lines 19-22), it now reads as “During this period of shrinkage, the observed mixing ratio of O_x largely decreased from 130 ppb to 80 ppb, and the observed OOA decreased from 16.2 μg m⁻³ to 11.4 μg m⁻³ (Fig. 4b, c). However, the concentrations of NH₄⁺ were almost constant. Repartition of the semivolatile SOA in gas and particle phases was hypothesized to cause the evaporation of semivolatile SOA to the gas phase.”

19) Page 12, Line 19 “then in”, “transience”: they should be corrected.

Response: Corrected.

20) Page 12, Line 26: Section 4.5 As I described above, this section is not so meaningful and should be removed. How did the author consider the contribution of primary particles in this analysis?

Response: Please see our comment 4) and more information presented below:

We used a high-time resolution PARALLELING particle sizer, i.e., FMPS, to measure the particle number size distribution (PNSD) in 1 s time resolution. The high time resolution of FMPS can allow clearly identify the signals of newly formed particles from preexisting ambient particles, e.g., freshly emitted particles from combustion, as well as the mixing process of the different types of particles (Liu et al., 2014; Man et al., 2015; Zhu et al., 2017, 2019).

According to our previous studies (e.g. Zhu et al., 2017, ACP) and the review paper by Tuan et al. (2015), the PNSD from traffic emissions are characterized by two peaks, i.e., about 16 nm and 30 nm, and intermittently last a few seconds or minutes (Figure R1). Figure R2 (added in new supporting information) shows the fresh industrial emissions associated with SO₂ and/or the cooking emissions associated with increased COA at 18:00-20:00. It is clear that the dominant modes of

particles from traffic emissions, industrial emissions and cooking emissions occurred at ~20 nm, ~30 nm and ~40 nm, respectively, and the domain mode size were quietly stable in the study period. Their contributions were important to the particle number concentrations during non-NPF periods, which were not the focus of this study. On the roof sampling site, their contributions to the observed particle concentrations during the initial few hours of NPF were generally negligible in presence of wind speeds of 4-6 m s⁻¹, except a few occasional spikes lasting in minutes. These spikes were excluded in calculating NMINP. In the revision, we add “Note that a few spikes of several minutes were occasionally observed and were excluded to calculate NMINP because they may reflect primary particles from localized sources (Liu et al., 2014; Zhu et al., 2017).” The same is true in calculating the growth rate of particles, shrinkage rate and D_{pgmax}. Additionally, their influences can also be ignored in studying the growth of newly formed particles when the particles grew over 50 nm.

During the NPF events (e.g. Figure R3), COA occasionally influences the new particles signal, and the growth of new particles was consistent with the increase in LO-OOA and MO-OOA. Therefore, we argued that the growth of new particles depends largely on the condensational growth.

We prefer to add the argument in Supporting Information since the challenge is not immediately related to the samplings and associated analyses presented in the text.

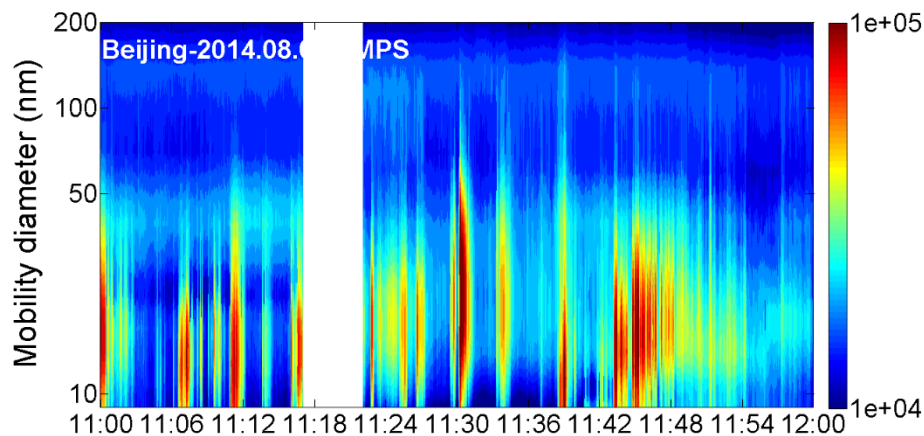


Figure R1 Contour plot of traffic emissions (a) and the raw FMPS data of the vehicle spikes (b).

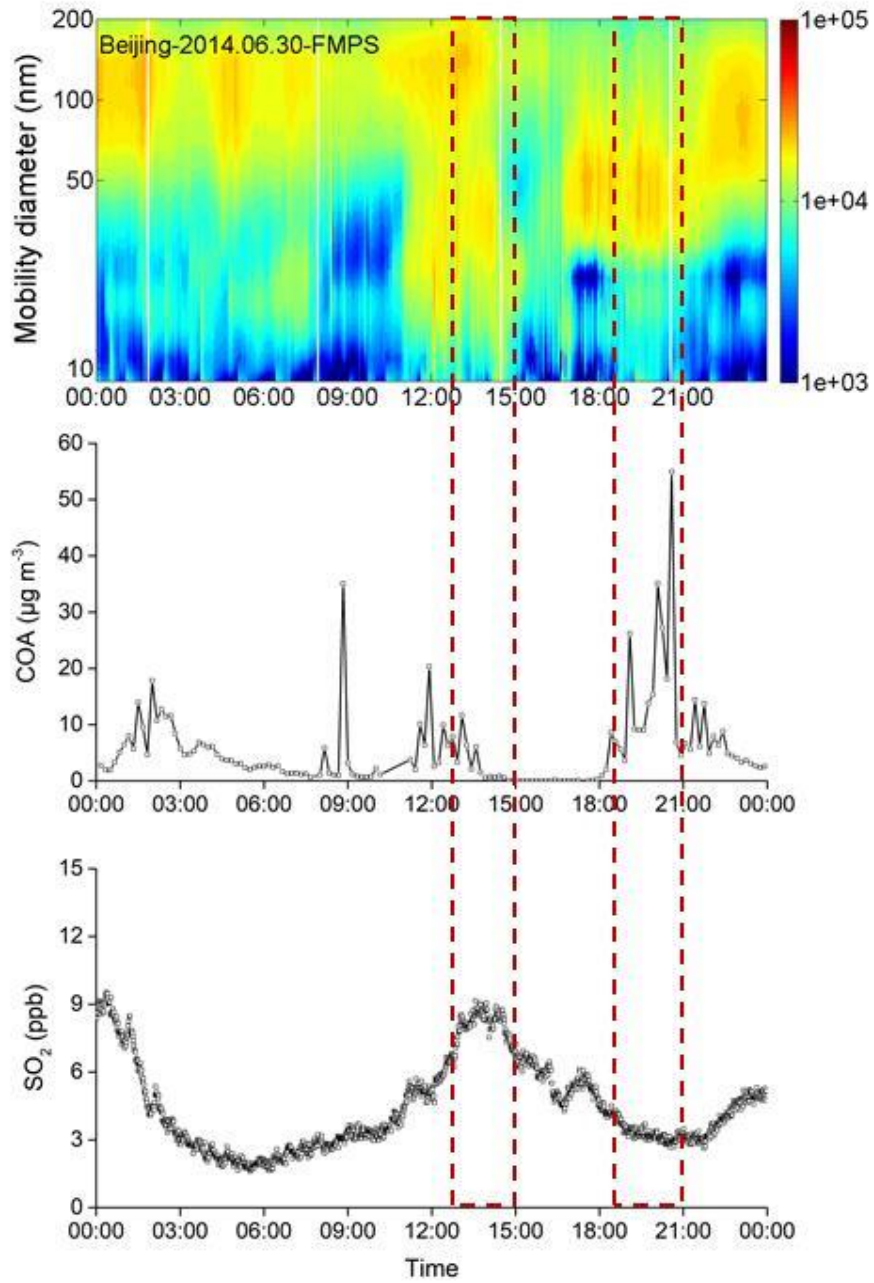


Figure R2 Fresh industrial emissions with high SO_2 (12:30-15:00) and the cooking emissions with increased cooking OA (COA, 18:20-21:00).

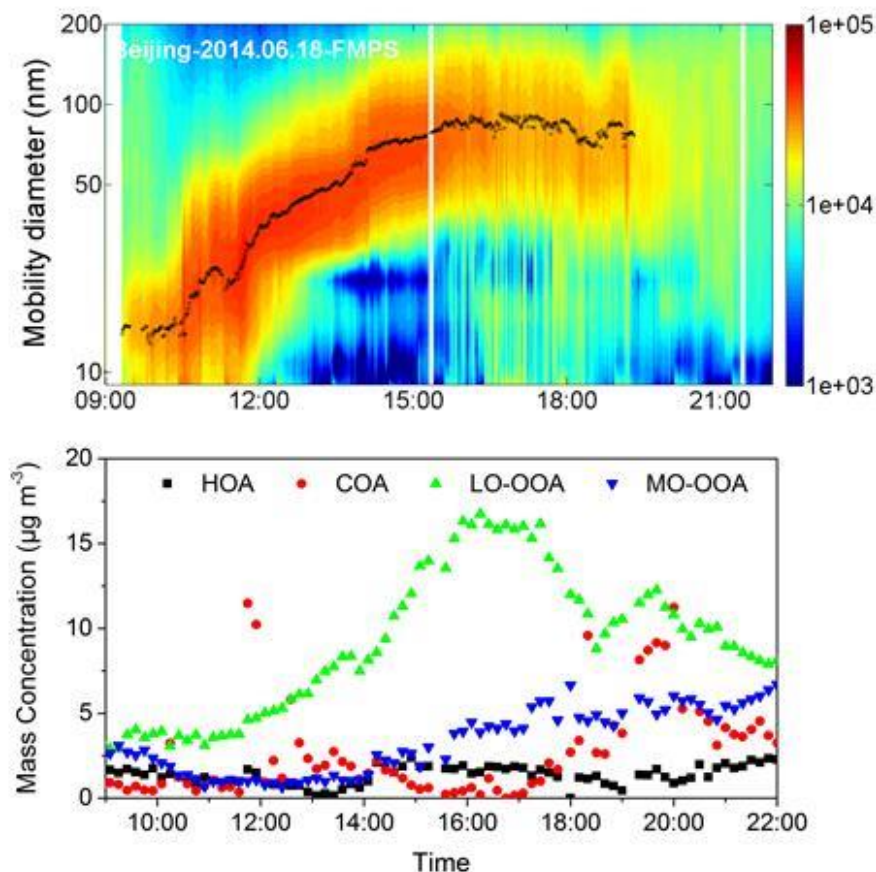


Figure R3 NPF event and the variations of hydrocarbon-like OA (HOA), cooking OA (COA), less oxidized oxygenated OA (LO-OOA) and more oxidized oxygenated OA (MO-OOA) on June 18, 2014.

Reference:

- Baek, J., Hu, Y.T., Odman, M.T., and Russell, A.G.: Modeling secondary organic aerosol in CMAQ using multigenerational oxidation of semi-volatile organic compounds, *J. Geophys. Res.*, 116, D22204, doi: 10.1029/2011JD015911, 2011.
- Brean, J., Harrison, Roy., Shi, Z., Beddows, D. C. S., Acton, W., Nicholas Hewitt, C., Squires, F. A., and Lee J.: Observations of highly oxidized molecules and particle nucleation in the atmosphere of Beijing, *Atmos. Chem. Phys.*, 19, 14933–14947, doi: 10.5194/acp-19-14933-2019, 2019.
- Burkart, J., Hodshire, A. L., Mungall, E. L., Pierce, J. R., Collins, D.B., Ladino, L. A., Lee, A. K., Irish, V., Wentzell, J. J., Liggio, J., and Papakyriakou, T.: Organic condensation and particle growth to CCN sizes in the summertime marine Arctic is driven by materials more semivolatile than at continental sites, *Geophys. Res. Lett.*, 44, 10725–10734, doi: 10.1002/2017GL075671, 2017.
- Chen, X., Yang, W., Wang, Z., Li, J., Hu, M., An, J., Wu, Q., Wang, Z., Chen, H., Wei, Y., Du, H., and Wang, D.: Improving new particle formation simulation by coupling a volatility-basis set (VBS) organic aerosol module in NAQPMS+APM, *Atmos. Environ.*, 204, 1–11, doi: 10.1016/j.atmosenv.2019.01.053, 2019.
- Chu, B., Kerminen, V. M., Bianchi, F., Yan, C., Petäjä, T., and Kulmala, M.: Atmospheric new particle formation in China. *Atmos. Chem. Phys.*, 19, 115-138, doi: 10.5194/acp-19-115-2019,

2019.

- Du, W., Zhao, J., Wang, Y., Zhang, Y., Wang, Q., Xu, W., Chen, C., Han, T., Zhang, F., Li, Z., Fu, P., Li, J., Wang, Z., and Sun, Y.: Simultaneous measurements of particle number size distributions at ground level and 260 m on a meteorological tower in urban Beijing, China, *Atmos. Chem. Phys.*, 17, 6797–6811, doi: 10.5194/acp-17-6797-2017, 2017.
- Ehn, M., Thornton, J.A., Kleist, E., Sipilä, M., Junninen, H., Pullinen, I., Springer, M., Rubach, F., Tillmann, R., Lee, B., Lopez-Hilfiker, F., Andres, S., Acir, I., Rissanen, M., Jokinen, T., Schobesberger, S., Kangasluoma, J., Kontkanen, J., Nieminen, T., Kurtén, T., Nielsen, L.B., Jørgensen, S., Kjaergaard, H.G., Canagaratna, M., Maso, M.D., Berndt, T., Petäjä, T., Wahner, A., Kerminen, V., Kulmala, M., Worsnop, D.R., Wildt, J., and Mentel, T.F.: A large source of low-volatility secondary organic aerosol, *Nature*, 506, 476–479, doi: 10.1038/nature13032, 2014.
- Guo, S., Hu, M., Zamora, M. L., Peng, J., Shang, D., Zheng, J., Du, Z., Wu, Z., Shao, M., Zeng, L., Molina, M. J., and Zhang, R.: Elucidating severe urban haze formation in China, *P. Natl. Acad. Sci. USA*, 111, 17373–17378, doi: 10.1073/pnas.1419604111, 2014.
- Guo, S., Hu, M., Peng, J., Wu, Z., Zamora, M. L., Shang, D., Du, Z., Zheng, J., Fang, X., Tang, R., Wu, Y., Zeng, L., Shuai, S., Zhang, W., Wang, Y., Ji, Y., Zhang, A., Wang, W., Zhang, F., Zhao, J., Gong, X., Wang, C., Molina, M., and Zhang, R.: Remarkable nucleation and growth of ultrafine particles from vehicular exhaust. *P. Natl. Acad. Sci.*, 117(7), 3427–3432, doi: 10.1073/pnas.1916366117, 2020.
- Knote C., Hodzic A., Jimenez J.L., Volkamer R., Orlando J.J., Baidar S., Brioude J., Fast J., Gentner D.R., Goldstein A.H., Hayes P.L., Knighton W.B., Oetjen H., Setyan A., Stark H., Thalman R., Tyndall G., Washenfelder R., Waxman E. and Zhang Q.: Simulation of semi-explicit mechanisms of SOA formation from glyoxal in aerosol in a 3-D model, *Atmos. Chem. Phys.*, 14, 6213–6239, doi:10.5194/acp-14-6213-2014, 2014.
- Kulmala, M., Petaja, T., Kerminen, V., Kujansuu, J., Ruuskanen, T., Ding, A., Nie, W., Hu, M., Wang, Z., Wu, Z., Wang, L., Worsnop, D. R. On secondary new particle formation in China. *Frontiers of Environmental Science & Engineering in China*, 10(5):08, doi: 10.1007/s11783-016-0850-1, 2016.
- Kulmala, M., Dal Maso, M., Mäkelä, J. M., Pirjola, L., Väkevä, M., Aalto P., Miikkulainen, P., Hämeri, K., O'dowd, C.D.: On the formation, growth and composition of nucleation mode particles, *Tellus*, 53B, 479–490, doi: 10.1034/j.1600-0889.2001.530411.x, 2001.
- Lee, S., Gordon, H., Yu, H., Lehtipalo, K., Haley, R., Li, Y., and Zhang, R.: New Particle Formation in the Atmosphere: From Molecular Clusters to Global Climate, *J. Geophys. Res. Atmos.*, 124, 7098–7146, doi: 10.1029/2018JD029356, 2019.
- Liu, X.H., Zhu, Y.J., Zheng, M., Gao, H.W., Yao, X.H. Production and growth of new particles during two cruise campaigns in the marginal seas of China. *Atmos. Chem. Phys.*, 2014, 14, 7941–7951.
- Lu, Y., Yan, C., Fu, Y., Chen, Y., Liu, Y., Yang, G., Wang, Y., Bianchi, F., Chu, B., Zhou, Y., Yin, R., Baalbaki, R., Garmash, O., Deng, C., Wang, W., Liu, Y., Petäjä, T., Kerminen, V., Jiang, J., Kulmala, M., and Wang, L.: A proxy for atmospheric daytime gaseous sulfuric acid concentration in urban Beijing, *Atmos. Chem. Phys.*, 19, 1971–1983, 2019.
- Man, H., Zhu, Y., Ji, F., Yao, X., Lau, N. T., Li, Y. J., Lee, B.P., Chan, C. K. Comparison of daytime and nighttime new particle growth at the HKUST Supersite in Hong Kong, *Environ. Sci. & Technol.*, 49 (12), 7170–7178, 2015.
- Matsui, H., Koike, M., Kondo, Y., Takegawa, N., Wiedensohler, A., Fast, J.D., Zaveri, R. A.: Impact of new particle formation on the concentrations of aerosols and cloud condensation nuclei around Beijing, *J. Geophys. Res. Atmos.*, 116, D19208, doi: 10.1029/2011JD016025, 2011.
- Riipinen, I., Pierce, J. R., Yli-Juuti, T., Nieminen, T., Häkkinen, S., Ehn, M., Junninen, H., Lehtipalo,

- K., Petäjä, T., Slowik, J., Chang, R., Shantz, N. C., Abbatt, J., Leaitch, W. R., Kerminen, V.-M., Worsnop, D. R., Pandis, S. N., Donahue, N. M., and Kulmala, M.: Organic condensation: a vital link connecting aerosol formation to cloud condensation nuclei (CCN) concentrations, *Atmos. Chem. Phys.*, 11, 3865–3878, doi: 10.5194/acp-11-3865-2011, 2011.
- Tuan, V., Delgado-Saborit, J. M., and Harrison, R. M.: Review: Particle number size distributions from seven major sources and implications for source apportionment studies. *Atmos. Environ.*, 114-132, 2015.
- Wang, Z. B., Hu, M., Sun, J. Y., Wu, Z. J., Yue, D. L., Shen, X. J., Zhang, Y. M., Pei, X. Y., Cheng, Y. F., Wiedensohler, A. Characteristics of regional new particle formation in urban and regional background environments in the North China Plain. *Atmos. Chem. Phys.*, 13, 12495-12506, 2013.
- Wang, Z.B., Hu, M., Pei, X.Y., Zhang, R.Y., Paasonen, P., Zheng, J., Yue, D.L., Wu, Z.J., Boy, M., and Wiedensohler, A.: Connection of organics to atmospheric new particle formation and growth at an urban site of Beijing, *Atmos. Environ.*, 103, 7-17, doi:10.1016/j.atmosenv.2014.11.069, 2015.
- Wang, M., Kong, W., Marten, R., He, X., Chen, D., Pfeifer, J., Heitto, A., Kontkanen, J., Dada, L., Kürten, A., Yli-Juuti, T., Manninen, H., Amanatidis, S., Amorim, A., Baalbaki, R., Baccarini, A., Bell, D., Bertozzi, B., Bräkling, S., Brilke, S., Murillo, U. C., Chiu, R., Chu, B., De Menezes, L.-P., Duplissy, J., Finkenzeller, H., Carracedo, L. G., Granzin, M., Guida, R., Hansel, A., Hofbauer, V., Krechmer, J., Lehtipalo, K., Lamkaddam, H., Lampimäki, M., Lee, C.P., Makhmutov, V., Marie, G., Mathot, S., Mauldin, R. L., Mentler, B., Müller, T., Onnela, A., Partoll, E., Petäjä, T., Philippov, M., Pospisilova, V., Ranjithkumar, A., Rissanen, M., Rörup, B., Scholz, W., Shen, J., Simon, M., Sipilä, M., Steiner, G., Stolzenburg, D., Tham, Y. J., Tomé, A., Wagner, A. C., Wang, D. S., Wang, Y., Weber, S.K., Winkler, P. M., Wlasits, P. J., Wu, Y., Xiao, M., Ye, Q., Zauner-Wieczorek, M., Zhou, X., Volkamer, R., Riipinen, I., Dommen, J., Curtius, J., Baltensperger, U., Kulmala, M., Worsnop, D. R., Kirkby, J., Seinfeld, J. H., El-Haddad, I., Flagan, R. C., and Donahue, N. M.: Rapid growth of new atmospheric particles by nitric acid and ammonia condensation, *Nature* 581, 184–189, doi: 10.1038/s41586-020-2270-4, 2020.
- Wehner, B., Wiedensohler, A., Tuch, T. M., Wu, Z. J., Hu, M., Slanina, J., and Kiang, C. S.: Variability of the aerosol number size distribution in Beijing, China: New particle formation, dust storms, and high continental background, *Geophys. Res. Lett.*, 31, L22108, doi: 10.1029/2004GL021596, 2004.
- Wiedensohler, A., Cheng, Y.F., Nowak, A., Wehner, B., Achtert, P., Berghof, M., Birmili, W., Wu Z.J., Hu, M., Zhu, T., Takegawa, N., Kita, K., Kondo, Y., Lou, S.R., Hofzumahaus, A., Holland, F., Wahner, A., Gunthe, S.S, Rose, D., Su, H., Pöschl, U.: Rapid aerosol particle growth and increase of cloud condensation nucleus activity by secondary aerosol formation and condensation: A case study for regional air pollution in northeastern china, *J. Geophys. Res.*, 114, D00G08, doi: org/10.1029/2008JD010884, 2009.
- Wu, Z., Hu, M., Liu, S., Wehner, B., Bauer, S., Maßling, A., Wiedensohler, A., Petäjä, T., Dal Maso, M., Kulmala, M. New particle formation in Beijing, China: Statistical analysis of a 1-year data set. *J. Geophys. Res.: Atmos.*, 112(D9), doi: 10.1029/2006JD007406, 2007.
- Wu, Z.J., Zheng, J., Shang, D.J., Du, Z.F., Wu, Y.S., Zeng, L.M., Wiedensohler, A., and Hu, M.: Particle hygroscopicity and its link to chemical composition in the urban atmosphere of Beijing, China, during summertime, *Atmos. Chem. Phys.*, 16, 1123-1138, doi: 10.5194/acp-16-1123-2016, 2016.
- Yue, D.L., Hu, M., Zhang, R.Y., Wang, Z.B., Zheng, J., Wu, Z.J., Wiedensohler, A., He, L.Y., Huang, X.F, Zhu, T. The roles of sulfuric acid in new particle formation and growth in the mega-city of Beijing. *Atmos. Chem. Phys.*, 10, 4953-4960, 2010.
- Zhang, R., Khalizov, A., Wang, L., Hu, M., and Xu, W.: Nucleation and Growth of Nanoparticles in the Atmosphere, *Chem. Rev.*, 112, 1957-2011, doi: 10.1021/cr2001756, 2012.

Zhu, Y., Li, K., Shen, Y., Gao, Y., Liu, X., Yu, Y., Gao, H., and Yao, X.: New particle formation in the marine atmosphere during seven cruise campaigns, *Atmos. Chem. Phys.*, 19, 89-113, 2019.

Zhu, Y., Yan, C., Zhang, R., Wang, Z., Zheng, M., Gao, H., Gao, Y., and Yao, X.: Simultaneous measurements of new particle formation at 1 s time resolution at a street site and a rooftop site, *Atmos. Chem. Phys.*, 17, 9469-9484, 2017.

Investigating three patterns of new particles growing to the size of cloud condensation nuclei in Beijing's urban atmosphere

Liya Ma^{1#}, Yujiao Zhu^{1, 2##}, Mei Zheng³, Yele Sun⁴, Lei Huang¹, Xiaohuan Liu¹, Yang Gao¹, Yanjie Shen¹, Huiwang Gao^{1, 5} and Xiaohong Yao^{1, 5*}

5 ¹Lab of Marine Environmental Science and Ecology, Ministry of Education, Ocean University of China, Qingdao 266100, China

²Environment Research Institute, Shandong University, Qingdao, Shandong 266237, China

³State Key Joint Laboratory for Environmental Simulation and Pollution Control, College of Environmental Sciences and Engineering, Peking University, Beijing 100871, China

10 ⁴State Key Laboratory of Atmospheric Boundary Layer Physics and Atmospheric Chemistry, Institute of Atmospheric Physics, Chinese Academy of Sciences, Beijing 100029, China

⁵Laboratory for Marine Ecology and Environmental Sciences, Qingdao National Laboratory for Marine Science and Technology, Qingdao, China

#Equally contributed to this work; Correspondence to: Xiaohong Yao and Yujiao Zhu (*xhyao@ouc.edu.cn,

15 zhuyujiao@sdu.edu.cn)

Abstract. The growth of newly formed particles with diameters from ~10 nm to larger sizes was investigated in Beijing's urban atmosphere during December 10–23, 2011, April 12–27, 2012, and June–August 2014. In 11 out of 27 new particle formation (NPF) events during June–August, the maximum geometric median diameter (D_{pgmax}) of newly formed particles exceeded 75 nm, and the grown new particles may contribute to the population of cloud condensation nuclei. In contrast, no apparent growth in new particles with $D_{pgmax} < 20$ nm was observed in all of the events in December, in approximately half of the NPF events in April and only 2 events during June–August. New particles observed in the latter NPF events were too small to be activated as cloud condensation nuclei. Apparent new particle growth with $D_{pgmax} \leq 50$ nm was observed in the remaining 18 NPF events. The 11 NPF events during June–August with D_{pgmax} exceeding 75 nm were analyzed in detail. The particle growth patterns can be clearly classified into three types: one-stage growth, and two-stage growth-A and growth-B. The one-stage growth pattern is characterized by a continuous increase in D_{pg} with $D_{pgmax} \geq 80$ nm (4 out of 11 NPF events), and the two-stage growth-A and growth-B patterns are characterized by no apparent growth and shrinkage of particles, respectively, in the middle 2–4 h of the growth period (7 out of 11 NPF events). Combining the observations of gaseous pollutants and measured (or modeled) concentrations of particulate chemical species, the three growth patterns were discussed in terms of the spatial heterogeneity of NPF, formation of secondary aerosols, and evaporation of semi-volatile particulates. Secondary organic species and NH_4NO_3 were argued to be two major contributors to the growth of new particles, but NH_4NO_3 likely contributed to growth only in the late afternoon and/or at nighttime.

1 Introduction

Atmospheric aerosol particles can be derived either from primary emissions, including various natural and

anthropogenic sources, or from secondary sources (Yao et al., 2005; Sabaliauskas et al., 2012; Vu et al., 2015; Seinfeld and Pandis, 2016; Quan et al., 2017; Zhu et al., 2019). Secondary sources are mainly related to atmospheric nucleation, followed by the growth of newly formed particles from ~1 nm to larger sizes; this phenomenon is conventionally referred to as a new particle formation (NPF) event (Kulmala et al., 2004; Kerminen et al., 2018). In recent decades, numerous studies have been conducted on NPF, including field measurements in various atmospheres, laboratory studies on nucleation and initial growth in newly formed particles, regional-scale modeling of NPF and its impacts on climate, and development of new techniques for analyzing the chemical components of nanoparticles and their gaseous precursors. Building on the results of these studies, many review papers have summarized the state-of-the-art progress and noted challenges for future studies (Kulmala et al., 2004, 2012, 2016; Kulmala and Kerminen, 2008; Zhang et al., 2012, 2015; Kerminen et al., 2018; Chu et al., 2019; Lee et al., 2019).

Several studies have investigated the potential climate impacts of NPF events, for example, 10% to 60% of NPF events have been reported to yield an appreciable contribution to cloud condensation nuclei (CCN) (Kuang et al., 2009; Asmi et al., 2011; Laakso et al., 2013; Yu et al., 2014; Rose et al., 2017; Kerminen et al., 2018). Modeling studies have also proposed that approximately 50% of the CCN population is attributable to NPF events in the troposphere (Yu and Luo, 2009; Yu et al., 2014; Gordon et al., 2017). Nevertheless, reported observations have also shown that newly formed particles with diameters less than 40–50 nm can be activated as CCN only under high supersaturation (SS), such as >0.6% (Li et al., 2015; Ma et al., 2016). When newly formed particles grow with the geometric median diameter to larger than 70 nm, they significantly contribute to the CCN population at SS ≤ 0.2% (Wiedensohler et al., 2009; Yue et al., 2011; Li et al., 2015; Ma et al., 2016; Zhu et al., 2019). In addition, field observations have also shown that in most NPF events, the maximum geometric median diameter (D_{pgmax}) of newly grown particles is less than 40–50 nm before new particle signals drop to a negligible level (Zhu et al., 2014, Liu et al., 2014; Man et al., 2015; Zhu et al., 2017; Yu et al., 2019). Thus, it is important to characterize NPF events, based on the D_{pgmax} of grown new particles, and to explore the chemicals driving the growth of newly formed particles with D_{pgmax} greater than 70 nm.

With distinctive particle growth patterns being widely reported, Beijing is an ideal area for studying the growth of newly formed particles (Wehner et al., 2004; Wu et al., 2007, 2016; Wiedensohler et al., 2009; Yue et al., 2010; Matsui et al., 2011; Wang et al., 2013; Guo et al., 2014, 2020; Du et al., 2017; Zhu et al., 2017; Brean et al., 2019; Chen et al., 2019). For instance, as the first study of NPF events in Beijing, Wehner et al. (2004) reported a small growth rate (~1 nm h⁻¹) of newly formed particles during 25 days from March 05 to April 18, 2004. Such small growth rates are unlikely to facilitate the growth of particles to reach CCN sizes prior to removal from ambient air because of the large coagulation loss in Beijing (Kulmala and Kerminen, 2008; Kulmala et al., 2016; Chu et al., 2019; Guo et al., 2020). Similar to this finding, no apparent growth of newly formed particles with the D_{pgmax} of approximately 10 nm always occurred in December 2011 at the same

campus in Beijing (Zhu et al., 2017). In contrast, the growth of newly formed particles to CCN size and even larger has also been observed in Beijing (Wu et al., 2007; Wiedensohler et al., 2009; Yue et al., 2010; Wang et al., 2013; Guo et al., 2014; Wu et al., 2016). The patterns of particle growth have not been well characterized. Nevertheless, sulfuric acid and/or organic vapors have been proposed to drive particle growth in different NPF events (Wiedensohler et al., 2009; Yue et al., 2010; Wu et al., 2016). Recently, the formation of NH_4NO_3 has been proposed as a driver of the rapid growth of newly formed particles in field studies and chamber experiments (Zhu et al., 2014; Man et al., 2015; Wang et al., 2020). The role of NH_4NO_3 in the growth of newly formed particles in Beijing remains poorly understood. Matsui et al. (2011) and Chen et al. (2019) simulated NPF and the growth of newly formed particles based on observations, but the modeling results were explained with large uncertainties.

In this study, we investigated NPF events in Beijing using observational data from three campaigns. We characterized NPF events according to the observed D_{pgmax} of newly formed particles and then focused on analyzing the growth patterns of newly formed particles with diameter from ~ 10 nm to a larger size, paying particular attention to NPF events in which the D_{pgmax} exceeded 70 nm. We combined observations of gaseous pollutants and observed (or modeled) concentrations of organic matter (or secondary organic aerosol, SOA), NO_3^- , and NH_4^+ , to identify the chemicals driving the growth of new particles, for example, varying major contributors in different growth periods. The survival probability of newly formed particles, which can grow over 50 nm or 70 nm (two CCN threshold sizes under different SS), was also estimated. Our study provides new insight into the growth of newly formed particles to larger sizes, as required for these particles to be activated as CCN at normal SS in the atmosphere.

2 Methods

2.1 Sampling periods, sites, and instruments

Two sampling sites were adopted to measure the particle number concentration spectra in Beijing. One is a rooftop site on the roof of an academic building within the campus of Peking University (39.99°N, 116.31°E, ~ 20 m above ground level); the other is a street site along a road located approximately 200 m from the rooftop site (Fig. 1). At the rooftop site, measurements were taken on December 16–23, 2011, April 12–27, 2012, and June 1–August 31, 2014. At the street site, measurements were taken on December 10–23, 2011 and April 18–27, 2012. The concentrations of atmospheric particles were measured using a fast mobility particle sizer (FMPS, TSI Model 3091) downstream of a dryer (TSI, 3091) at a one-second time resolution in each measurement campaign. The FMPS was a paralleling particle sizer and reported number size distributions of aerosol particles from 5.6 nm to 560 nm. In this study, the empirical correction procedure for FMPS size distribution data proposed by Zimmerman (2015) was used for correction. The scaling-down coefficient of the total particle number concentration measured by the FMPS (1.28) was obtained through a correlation analysis of side-by-side measurements made by the FMPS and a condensation particle counter (CPC). A SO_2 analyzer (Thermo Model 43i), an O_3

analyzer (Thermo Model 49i), a NO_x analyzer (Thermo Model 42i), and a meteorological monitoring system were operated at a one-minute resolution to obtain real-time observational data of gases and meteorological parameters on the rooftop site close to the FMPS in 2011, 2012, and before July 10, 2014. During the other observational periods (July 11–August 31, 2014), the mixing ratios of air pollutants at a one-hour resolution and meteorological data at a three-hour resolution were taken from the Wanliu Air Quality Monitoring Station in Haidian district (39.99°N, 116.32°E, <http://106.37.208.233:20035/>) and the Beijing 54511 station (39.95°N, 116.30°E, <https://rp5.ru/>), respectively. The concentrations of oxygenated organic aerosols (OOA) and inorganic species including NO₃⁻, SO₄²⁻, and NH₄⁺ in PM_{1.0}, during the period from June 3–July 11, 2014, previously reported by Xu et al. (2017), were also used to facilitate the analysis. The data were measured using a High-Resolution Time-of-Flight AMS (HR-ToF-AMS) at 10 min resolution. The chemical composition of PM_{1.0} measured by AMS has been widely used to interpret NPF events in the literature (Wiedensohler et al., 2009; Zhang et al., 2014; Man et al., 2015; Du et al., 2017; Rodelas et al., 2019; Kanawade et al., 2020) and was also used in this study. Low loadings of particulate chemical species in nanometer size ranges do not facilitate accurate measurement of their concentrations therein. However, the chemical composition of nanometer particles may differ from those of PM_{1.0} (Ehn et al., 2014; Wu et al., 2016). Moreover, the sampling site of the HR-ToF-AMS was located at the Tower branch of the Institute of Atmospheric Physics in Beijing, China (39.98°N, 116.38°E), and approximately 8 km away from Peking University. During NPF events at wind speeds of 4–6 m s⁻¹, a half-hour delay may occur for air parcels sweeping from one site with the FMPS deployed to another site with the AMS deployed. For NPF events with durations over several hours, the events were expected to occur regionally (Kerminen et al., 2018; Chu et al., 2019). Thus, it is reasonable to interpret the cumulative growth of newly formed particles within several hours, measured by the FMPS, by using the net simultaneous change in concentrations of chemical species, measured by the AMS. Additionally, He et al. (2001) reported that the chemical composition of PM_{2.5} was reasonably homogeneous in the two sampling site zones.

2.2 Computational methods

NPF events were identified according to the definition by Dal Maso et al. (2005), and only NPF events with durations over one hour were analyzed in this study. The local standard time was used to describe the NPF events in this study. In each NPF event, the net maximum increase in the nucleation mode particle number concentration (NMINP) was calculated according to Zhu et al. (2017). The nucleation mode was defined from 8 to 20 nm in this study.

$$\text{NMINP} = N_{8-20 \text{ nm}}(t_1) - N_{8-20 \text{ nm}}(t_0) \quad (1)$$

$N_{8-20 \text{ nm}}$ represents the sum of particle number concentrations with diameters from 8 nm to 20 nm; t_0 and t_1 represent the time of the initial observation of an NPF event and the time at which $N_{8-20 \text{ nm}}$ arrives at the maximum value, respectively. Note that a few spikes of several minutes were occasionally observed and were excluded to calculate NMINP because they may reflect primary particles from localized sources (Liu et al., 2014; Zhu et al., 2017).

The growth rate (GR) and shrinkage rate (SR) of new particles are determined by the slope of the fitted geometric median diameter of new particles (D_{pg}) over time (Whitby et al., 1978; Yao et al., 2010; Zhu et al., 2014; Man et al., 2015). In an NPF event or in each growth period of one NPF event, the maximum value of D_{pg} is defined as D_{pgmax} . Again, a few occasional spikes of several minutes were excluded to calculate GR, SR, and D_{pgmax} (Liu et al., 2014; Zhu et al., 2017).

5 Lu et al. (2019) recently developed an equation to estimate the gaseous sulfuric acid concentration in Beijing. The equation is expressed as follows:

$$[H_2SO_4] = 280.05 \cdot UVB^{0.14} \cdot [SO_2]^{0.40} \quad (2)$$

The units for $[H_2SO_4]$ and $[SO_2]$ are molecule cm^{-3} , and the unit for UVB (ultraviolet B) is $W m^{-2}$. The reported error was within 20% for the calculated concentrations against the observations in Beijing (Lu et al., 2019). UVB occupies 5% of the ultraviolet radiation that reaches the Earth's surface (https://en.wikipedia.org/wiki/Ultraviolet#cite_note-Skin_Cancer_Foundation-23). Thus, UVB values were obtained by multiplying the downward ultraviolet radiation at the surface by 5% in this study, and the ultraviolet radiation data were downloaded from the Climate Data Store (<https://cds.climate.copernicus.eu/>). The contribution of sulfuric acid vapor to particle growth was calculated based on the method reported by Kulmala et al. (2001) and Nieminen et al. (2010).

$$15 \quad R = ([H_2SO_4]_{avg}/C) \times 100\% \quad (3)$$

where $[H_2SO_4]_{avg}$ is the average concentration of H_2SO_4 vapor during the particle growth period, and C is the total concentration of condensable vapor for the particle growth. Here, the surface vapor pressure of the condensable material is assumed to be zero, and C can be calculated based on the equation of Kulmala et al. (2001).

$$C = \rho \left\{ \frac{D_{pg2}^2 - D_{pg1}^2}{2} + \left[\frac{4}{3a} - 0.623 \right] \lambda (D_{pg2} - D_{pg1}) + 0.623 \lambda^2 \ln \frac{\lambda + D_{pg2}}{\lambda + D_{pg1}} \right\} / \Delta t D m \quad (4)$$

20 ρ is the particle density in $g cm^{-3}$, a is the mass accommodation coefficient (i.e., sticking probability), λ is the mean free path in nm, Δt (s) is the time during particle growth from D_{pg1} to D_{pg2} , D ($cm^2 s^{-1}$) is the diffusion coefficient of the condensing vapor, and m is the molecular mass of the condensable vapor in $g mol^{-1}$.

When D_{pg} of the grown new particles reached 50 nm, the survival probability (SP) of grown new particles at $D_{pg} = 50$ nm was estimated as:

$$25 \quad SP = \frac{N_{50+3\sigma}}{N_{MINP}} \times 100\% \quad (5)$$

where σ represents the standard deviation of the median diameter in the fitted log-normal distribution of grown new particles, and 3σ covering 99% of the mode particles. $N_{50+3\sigma}$ refers to the integral value of the number concentration of new particles with diameters from 50 nm to $50 + 3\sigma$ nm.

We further defined another technical term, that is, two times the SP ($2*SP$). The final SP was between SP and $2*SP$ because some new particles with diameters from $50 - 3\sigma$ nm to 50 nm may eventually grow over 50 nm with an increase in

D_{pg} . However, the amount of new particles with diameters from $50 - 3\sigma$ nm to 50 nm that can grow over 50 nm varies case by case, which is also applicable to the final SP. Similar definitions are applied for the SP of grown new particles with D_{pg} reaching over 70 nm, in which grown new particles can be activated as CCN with highly variable activation efficiencies. Note that the observed number concentrations of newly grown particles with a larger size sometimes exceeded those with a smaller size under the condition of spatial heterogeneity of NPF. In these cases, that is, NPF events occurring on June 23, and August 12 and 15, SP was not calculated.

The amount of chemical species required to grow new particles from D_{pg1} to D_{pg2} ($Mass_{required}$) is approximately estimated as follows:

$$Mass_{required} = 4/3\pi [(D_{pg2}/2)^3 - (D_{pg1}/2)^3] * N * \rho \quad (5)$$

ρ is the density, which is assumed as $1.5 \mu\text{g m}^{-3}$ for OOA (or SOA) and $1.7 \mu\text{g m}^{-3}$ for NH_4NO_3 , respectively. Considering that the particle number concentration may decrease because of the dry deposition, diffusion and dilution effects, and particle coagulation, N represents the integral value of new particle number concentrations with the geometric median diameter of new particles from $D_{pg2-3\sigma}$ to $D_{pg2+3\sigma}$. The approximate value may overestimate the required amount because particle-particle coagulation has not been deducted.

2.3 Model description

The U.S. EPA Community Multiscale Air Quality Model (CMAQ version 5.0.2, Byun and Schere, 2006) was applied to simulate inorganic ions such as NO_3^- , SO_4^{2-} , NH_4^+ , and SOA in $\text{PM}_{2.5}$ over East Asia. Fig. S1 shows the nested domains, with the 36 km domain 1 (d01) and the 12 km domain 2 (d02) over eastern China and China adjacent seas. The vertical resolution includes 14 logarithmic structure layers from the surface to the tropopause, with the first model layer height of 36 m above the ground level. Meteorological fields were generated by the Weather Research and Forecasting (WRF) Model (v3.7). The initial and boundary conditions were obtained from the National Center for Environmental Prediction (NCEP) FNL (Final Operational Global Analysis datasets (<http://rda.ucar.edu/datasets/ds083.2>)). The major physics options included the Lin microphysics scheme, RRTM long-wave radiation scheme, Goddard short wave scheme, Monin-Obukhov surface-layer scheme, thermal diffusion land-surface scheme, and YSU land-surface scheme. The WRF hourly output files were processed using the Meteorology-Chemistry Interface Processor (MCIP v4.3). In CMAQ, the CB05tucl chemical mechanism module coupled with AERO6 was used to simulate the concentrations of gases and aerosols. Initial conditions (ICONS) and boundary conditions (BCONS) of pollutants in d01 were generated using the results from a global chemistry model of GEOS-Chem, while ICONS and BCONS for d02 were obtained from the results of d01. The Multi-resolution Emission Inventory for China (MEIC) in 2014, developed by Tsinghua University (<http://www.meicmodel.org/>), combined with BVOC emissions generated from Gases and Aerosols from Nature (MEGAN v 2.0.4, Guenther et al., 2006) was used in this

study. A spin-up time of five days was used to minimize the influence of ICONs.

Liu et al. (2010 a, b), Qi et al. (2018), and Zhang et al. (2019) reported the validation of the CMAQ application in China, in which good agreements between the simulated and measured concentrations of particulate components were generally obtained. During the study period, the model results generally met the benchmark criteria of the above four species (US-EPA, 2007), with correlations between modeled and measured values larger than 0.57 (Table S1). The modeled concentrations of NH_4^+ reasonably agree with the observations with a normalized mean bias (NMB) of 6%. The NMB slightly increased up to 12% for the modeled concentrations of SO_4^{2-} . The modeled values of NO_3^- and SOA were underestimated with NMBs of -29% and -39%, respectively. Underestimation of SOA is a common weakness of the model simulation because a fraction of SOA precursors are not included, and some key formation pathways of SOA may still be missing in current air quality models (Baek et al., 2011; Knote et al., 2014). Detailed evaluation results of this study are provided in the Supporting Information.

3. Results

3.1 Overview of NPF events in three campaigns

A total of 46 NPF events were observed during the three campaigns in Beijing, and the occurrence frequencies of NPF events decreased clearly in the rainy season (Table 1, Fig. S2). In Campaign 1, seven NPF events were observed during December 10–23, 2011 (7 out of 14) at the street site. During December 16–23, three NPF events were observed (3 out of 8) at the rooftop site, which occurred simultaneously with the events at the street site. In Campaign 2, seven NPF events were observed at the rooftop site during April 12–27, 2012 (7 out of 16). During April 18–27, 2012, two NPF events were observed at the street site simultaneously with the events observed (2 out of 10) at the rooftop site. In Campaign 3, 13 NPF events occurred in June out of a total of 30 observational days. The occurrence frequency decreased to approximately 20% in July and August (seven NPF events from 31 observational days). Beijing enters the rainy season in July and August, and the weather conditions are unfavorable for NPF events (Wu et al., 2007).

The NMINP varied largely from event to event in the five months, but the monthly averages were generally closer to each other. For example, the monthly average values were $1.5 \pm 0.8 \times 10^4 \text{ cm}^{-3}$ (average value \pm standard deviation) in June 2014 and $1.6 \pm 0.8 \times 10^4 \text{ cm}^{-3}$ in July and August 2014. The large values of NMINP implied the NPF to be an important source of ambient particles when particle number concentrations were considered. The NMINP was $1.6 \pm 0.7 \times 10^4 \text{ cm}^{-3}$ at the rooftop site in April 2012, but it was lower ($1.3 \pm 0.2 \times 10^4 \text{ cm}^{-3}$) at the street site. In December 2011, the NMINP was only $8.3 \pm 4.2 \times 10^3 \text{ cm}^{-3}$ at the rooftop site, but it was still $1.5 \pm 0.7 \times 10^4 \text{ cm}^{-3}$ at the street site. There was no significant difference in the NMINP at the rooftop site between April and June–August, but the values in the four months were significantly larger than those at the rooftop site in December ($P < 0.05$). Zhu et al. (2017) discussed the seasonal difference in the NMINP between the two nearby sites in terms of the effects of the condensation sink and low temperature.

3.2 Season-dependent growth patterns of newly formed particles

As reported by Dusek et al. (2006), atmospheric particles with a diameter below 60 nm were unlikely to be activated as CCN at a normal SS, such as $\leq 0.2\%$. Investigating the growth behaviors of newly formed particles, three growth patterns, Classes I, II, and III, were identified on the basis of their potentials to act as CCN at normal SS (Figs. 2–4 and Figs. S3–6). Class I was characterized by no apparent particle growth. For example, the fitted D_{pg} of new particles was almost constant at 11 nm for ~ 10 h on April 25, 2012, until the new particle signal dropped to a negligible level (Table 1, Fig. S3a). The new particles unlikely grew to CCN size prior to removal from ambient air.

Class II was characterized by the fitted D_{pg} of new particles growing from 10 ± 2 nm to 20–50 nm, as shown in Fig. S3b–e. Class II can be further subclassified into four scenarios. In Scenario 1, the new particle growth lasted for a few hours with D_{pg} increasing to 27–48 nm, after which it stopped (Fig. S3b). The increased size was maintained for a few hours until the new particle signal dropped to a negligible level. The growth of newly formed particles seemingly encountered a ceiling in Scenario 1, in which new particles grown at the maximum D_{pg} unlikely contributed to CCN at normal SS. The ceiling prevented newly formed particles from growing to the CCN size in Scenario 1. The possibility of new particles to grow to CCN size in Scenarios 2–4 remains unknown. For example, new particles grew with D_{pg} approaching 32–45 nm in Scenario 2. Afterwards, the signal of the new particles was apparently replaced by another signal of the new particles with an obviously smaller diameter (Fig. S3c). In Scenario 3, new particles grew with D_{pg} increasing to 20–50 nm, and the new particle signal was overwhelmed by aged plumes. In the half or one hour switching from new particle signals to aged plume signals, D_{pg} rapidly increased by dozens of nanometers (Fig. S3d), similar to those reported by Man et al. (2015). Scenario 3 was quite common in the presence of air pollutant plumes (Levy et al., 2013; Zhang et al., 2015). In Scenario 4, the D_{pg} of new particles increased to 31–50 nm. Afterwards, no data were available to judge any further particle growth (Fig. S3e).

In Class III, the D_{pg} of new particles experienced either a continuous increase or a noncontinuous increase with the final D_{pgmax} closer to 75–120 nm (Figs. 2–4 and Figs. S4–6). Class III can be further classified into three growth patterns, which will be detailed in later sections. In addition to particle size, various factors such as chemical composition, particle mixing states, and meteorological conditions may also largely affect CCN activation of aerosols with D_{pg} beyond 70 nm (Ma et al., 2016; Rose et al., 2017; Lee et al., 2019). Although new particles in Class III can grow to the CCN size, the CCN activation of grown new particles has been reported to vary case by case (Wiedensohler et al., 2009; Yue et al., 2011; Li et al., 2015; Ma et al., 2016). Overall, the D_{pgmax} of grown new particles increased from Class I to Class III.

In December, all of these observed NPF events (three NPF events at the rooftop site plus seven NPF events at the street site) were subject to Class I (Table 1, Fig. S2a). In April, 3 out of 7 NPF events at the rooftop site and three NPF events simultaneously observed at the street site were subject to Class I. The remaining 4 NPF events at the rooftop site in April were subject to Class II, of which half belonged to Scenarios 3 and 4 (Table 1, Fig. S2b). In June–August, a total of 2, 14,

and 11 out of 27 NPF events were subject to Class I, Class II, and Class III (Table 1, Fig. S2c-e), respectively. Newly formed particles in the summer appeared to have a high probability of growing to the CCN size, at least in 11 out of 27 NPF events. On the other hand, newly formed particles in the winter were unlikely to act as a potential source of CCN because their D_{pgmax} reached only 11 ± 1 nm. The occurrence probability of Class I events largely decreased in April and summer, with three Class I NPF events in April, no Class I NPF event in July, and one Class I NPF event each in June and August (Table 1, Fig. S2c-e). Additionally, the lack of Class III NPF events in April implied that newly formed particles were less likely to grow to the CCN size at normal SS.

Overall, the growth patterns of newly formed particles are strongly season-dependent, with a generally larger D_{pgmax} in June–August. The mechanisms for the growth of newly formed particles to the CCN size in Class III are thus critical for understanding the importance of grown new particles acting as a potential source of CCN at normal SS. The new particle growth behaviors in Class III NPF events were thus analyzed in further detail, and SPs of grown particles with D_{pgmax} at 50 nm and 70 nm were also estimated.

3.3 Growth patterns of newly formed particles reaching CCN size

Analyzing the observational results for June, July, and August 2014 separately, the occurrence frequencies of Class III NPF events in the three months were found to be very close to each other, with 4, 3, and 4 in June, July, and August, respectively. The 11 NPF events can be further classified into three particle growth patterns: one-stage particle growth, two-stage particle growth-A, and two-stage particle growth-B.

The one-stage particle growth pattern occurred in 4 out of 11 NPF events, in which the fitted D_{pg} of newly formed particles continuously increased from 11 nm to 80–100 nm in 6–17 h on June 18, July 12–13, and August 25, 2014 (Fig. 2, Fig. S4). The growth of new particles stopped at ~24:00 in 3 out of 4 NPF events, while it stopped as early as ~16:00 in the last event.

Of the 11 NPF events, 4 events exhibited the two-stage particle growth-A pattern. The initial D_{pg} of newly formed particles varied from 9 nm to 22 nm in different events, in which the particles grew to a larger size in the daytime, then oscillated for several hours, and eventually restarted the increase at night (Fig. 3, Fig. S5). In 2 out of 4 events, the increase in the D_{pg} of newly formed particles stopped for 2–3 h in the middle period and then resumed to reach up to 75 nm at 22:00. In the other 2 out of 4 events, D_{pg} remained unchanged for ~4 h in the middle period and then increased, reaching up to 110–115 nm at 1:00 the next day.

A total of 3 out of 11 NPF events exhibited the two-stage particle growth-B pattern, in which the D_{pg} of newly formed particles increased from 10–19 nm to 36–79 nm, then decreased to 24–50 nm in the next 2–4 h, and D_{pg} increased again, reaching up to 84–120 nm (Fig. 4, Fig. S6). In two events, the decrease in newly formed particles occurred at approximately 18:00, for example, D_{pg} from 78 nm to 52 nm at 18:00–21:22 on June 23 and D_{pg} from 57 nm to 35 nm at 17:50–20:30 on

July 26. However, the shrinkage occurred as early as 15:20–17:20 on June 11 with D_{pg} from 38 nm to 24 nm.

4 Discussion

4.1 One-stage new particle growth to CCN size

Among the four one-stage growth NPF events, newly formed particles took the shortest time to reach the maximum size on June 18, 2014 (Fig. 2a). The NPF event was first observed at 09:20, lasting for 11 h. From 09:20 to 10:36, no apparent growth in newly formed particles was observed. The concentrations of gaseous precursors during that period may have been too low to cause a detectable growth in new particles with diameters >10 nm, similar to the observations reported in Hong Kong by Man et al. (2015). After 10:36, the D_{pg} of newly formed particles increased from 14 nm to 88 nm at 15:54 with a particle growth rate of 14 nm h^{-1} . The ambient relative humidity (RH) was approximately 40% with an ambient temperature of approximately $30 \text{ }^\circ\text{C}$ (Fig. 2d), implying dry and hot conditions during the particle growth period. The observed mixing ratio of O_x ($\text{NO}_2 + \text{O}_3$) largely increased from ~ 60 ppb to ~ 130 ppb during the growth period, supporting the photochemical formation of secondary species to drive particle growth.

As mentioned above, the growth of newly formed particles is mainly attributed to sulfuric acid, ammonium nitrate, and secondary organic compounds (Wiedensohler et al., 2009; Riipinen et al., 2011; Zhang et al., 2012; Ehn et al., 2014; Man et al., 2015; Wang et al., 2015; Burkart et al., 2017; Lee et al., 2019; Wang et al., 2020). We therefore explore their respective contributions as follows. First, we calculated the contribution of sulfuric acid to the growth based on the observed mixing ratio of SO_2 and Equations 2–4. Second, we examined whether NH_4NO_3 freshly formed in $\text{PM}_{1.0}$ or $\text{PM}_{2.5}$ during the particle growth period. In case of no NH_4NO_3 formation, its contribution would not be expected. This is because an even higher product of $\text{HNO}_{3\text{gas}} * \text{NH}_{3\text{gas}}$ is required to overcome the kelvin effect and form NH_4NO_3 in nucleation mode and Aitken mode particles. Thus, the growth unexplained by sulfuric acid should be mainly contributed by SOA. Third, in case of NH_4NO_3 formation, we compared the net increase in NH_4NO_3 with that in SOA. It is noteworthy that this approach is limited by the uncertainty in explaining the growth because the ratios of increased NH_4NO_3 over increased SOA in $\text{PM}_{1.0}$ or $\text{PM}_{2.5}$ may not be the same as the ratios in nucleation mode and Aitken mode particles. In this case, the required mass of NH_4NO_3 or SOA to the growth was also estimated and compared with their respective net increases to facilitate the analysis.

Based on the observed mixing ratio of SO_2 and Equations 2–4, sulfuric acid was estimated to contribute $< 2\%$ to particle growth during the whole NPF period (Fig. 2b). Almost constant concentrations of NO_3^- and NH_4^+ were observed at 11:00–14:00, implying that fresh NH_4NO_3 formation did not occur before 14:00 (Fig. 2c). Therefore, SOA was the dominant contributor to particle growth before 14:00, as supported by the decrease in the hygroscopicity parameter of 50 nm atmospheric particles from ~ 0.3 to ~ 0.1 during the same event, independently reported by Wu et al. (2016). From 14:00 to 16:00, the concentrations of NO_3^- and NH_4^+ significantly increased, accompanied by an increase in OOA by $11 \mu\text{g m}^{-3}$. Assuming an increase in NO_3^- because of the formation of NH_4NO_3 , the net increase in NH_4NO_3 was $10 \mu\text{g m}^{-3}$. Thus, the

formation of NH_4NO_3 may also play an important role in the growth of new particles after 14:00. Zhu et al. (2014) and Man et al. (2015) reported that NH_4NO_3 can be an important contributor to the growth of new particles (from 40–50 to nm to a larger size at night). Supposing that the particle growth during the entire growth period from 11:00 to 16:00 was completely driven by SOA, the required amount was estimated as $8.9 \mu\text{g m}^{-3}$. The observed concentration of OOA in $\text{PM}_{1.0}$ increased by $15.5 \mu\text{g m}^{-3}$ during the growth period, which could reasonably satisfy the required amount. Note that only secondary organic compounds of low volatility can support the growth of small particles, and those of high volatility may also contribute to the growth of large particles (Ehn et al., 2014; Burkart et al., 2017). The growth of new particles stopped after 15:54 until the new particle signal gradually disappeared at ~20:00. The observed concentrations of OOA and NO_3^- did not increase during the four hours, although they largely oscillated.

Another example of one-stage growth occurred on August 25, 2014, and newly formed particles took the longest time to reach D_{pgmax} (Fig. 2e). RH was lower than 50%, and the ambient air temperature varied from 24°C to 31°C during the growth period (Fig. 2h), also indicating dry and hot conditions during the particle growth period. The NPF event was observed from 07:50 on August 25, 2014 to 08:00 the next day. The new particle signal was unstable in the initial three hours because of the spatial heterogeneity of NPF.

The D_{pg} of newly formed particles started to increase from 12 nm at 10:48 to 80 nm at 24:00 with a particle growth rate of 5.1 nm h^{-1} . During the period of 11:00–19:00, sulfuric acid contributed to only 6% of the increase in D_{pg} from 12 nm to 51 nm on the basis of the observed mixing ratios of SO_2 . Because of the lack of photochemical reactions, sulfuric acid concentrations should have been much lower during nighttime than during daytime (Petäjä et al., 2009; Lu et al., 2019).

No measured concentrations of particulate chemical species were available on that day. Their modeled concentrations in $\text{PM}_{2.5}$ were alternatively used to argue possible contributors to the growth of newly formed particles, although the uncertainty may be even larger than the use of measured particulate species in $\text{PM}_{1.0}$. The modeled concentrations of NH_4^+ and NO_3^- were almost constant at 11:00–18:00 (Fig. 2g), suggesting that NH_4NO_3 was did not freshly form to drive particle growth. Thus, SOA likely acted as the dominant contributor to particle growth.

The modeled net increase in particulate NH_4NO_3 was $3.6 \mu\text{g m}^{-3}$ from 18:00 to 22:00, with the D_{pg} of newly formed particles increasing from 47 nm to 70 nm (Fig. 2g). Assuming that the new particle growth from 18:00 to 22:00 was completely driven by NH_4NO_3 , the required amount was estimated to be $3.1 \mu\text{g m}^{-3}$. The modeled concentrations of SOA increased by $0.6 \mu\text{g m}^{-3}$ (Fig. 2g). Based on the modeled results, both NH_4NO_3 and SOA may have contributed significantly to particle growth in this period. The D_{pg} of newly formed particles increased from 70 nm to ~80 nm from 22:00 to 24:00 when the modeled concentrations of all species decreased because of the dilution effect. Afterwards, the new particles stopped growing until their signal gradually disappeared at 08:00 on the next day. The modeled concentrations of SOA and NH_4NO_3 were almost constant after 1:00 the next day, consistent with the lack of apparent growth in these large new

particles.

During the two NPF events on July 12 and 13, sulfuric acid vapor was estimated as a minor contributor to particle growth (Fig. S4). The modeled results suggested that both NH_4NO_3 and SOA were important contributors to particle growth, but NH_4NO_3 contributed to growth only at nighttime (Fig. S4c, Fig. S4g). Nevertheless, the concentrations of chemical species in nanometer particles of various sizes are required to confirm this.

4.2 Two-stage new particle growth-A to CCN size

Fig. 3 and Fig. S5 show that the final D_{pgmax} values of newly formed particles were 75 nm, 115 nm, 75 nm, and 110 nm on June 27, and August 6, 12 and 15, 2014, respectively. On June 27, 2014 (Fig. 3a-d), the NPF events were first observed at 09:00 and lasted for 18 h, with RH generally lower than 40%. Apparent growth of newly formed particles could not be observed from 09:00 to 10:30. The D_{pg} of newly formed particles increased from ~10 nm at 10:30 to 35 nm at 15:20, with a GR of 5.2 nm h⁻¹. Using the observed mixing ratio of SO₂, sulfuric acid vapor was estimated to contribute to the first-stage particle growth by 3% (Fig. 3b). The constant concentrations of NO₃⁻ observed during this period implied that NH_4NO_3 did not freshly form (Fig. 3c). Again, particle growth during the period, which could not be explained by sulfuric acid, should be completely driven by SOA. The required amount of SOA was estimated to be as low as 0.56 μg m⁻³. The observed OOA fluctuated at 5–6 μg m⁻³ during that period (Fig. 3c).

After 15:20, the D_{pg} of newly formed particles stopped growing and fluctuated at approximately 35 nm for approximately two hours. The first-stage particle growth apparently encountered an upper limit. Compared with the concentrations observed before and after the two-hour period, the significantly decreased number concentrations of newly formed particles imply spatial heterogeneity of NPF on that day. In other words, much weaker atmospheric nucleation generated new particles in the upwind atmosphere within a certain spatial range, and the grown new particles at a lower number concentration were transported and observed at the rooftop site at 15:20–17:40. The slightly decreased mixing ratios of O_x during this time, which were unexpected considering a sharp increase in the observed O_x after the period, imply reduced photochemical reaction activities in the upwind atmosphere at certain spatial ranges. The photochemical reaction activities during this period may be too weak to generate sufficient amounts of secondary organic and inorganic precursors to support the growth of new particles >35 nm to a larger size, and thus the growth encountered the upper limit, as shown in the diagram in the graphical abstract.

After 17:40, the D_{pg} of newly formed particles started to increase from 32 nm to 75 nm at 22:30, with a GR of 9.7 nm h⁻¹, which nearly doubled the growth rate observed during the first growth stage. The observed mixing ratio of O_x increased from 66 ppb at 17:20 to ~90 ppb at 21:20, supporting the secondary formation of chemical species to drive particle growth (Fig. 3b). The observed concentrations of OOA (left axis) and NO₃⁻ (right axis) rapidly increased from 18:00 to 22:20, with the former being approximately four times larger than the latter. The required amount of NH_4NO_3 for particle growth during

the period was estimated to be $5.3 \mu\text{g m}^{-3}$, while the net increase in NH_4NO_3 was $1.6 \mu\text{g m}^{-3}$. SOA may dominate the growth of new particles. Lee et al. (2016) and Huang et al. (2019) recently reported that highly functionalized organonitrates generated from the reaction of NO_3 free radicals with organics can contribute to the growth of particles at nighttime. After 22:30, the new particles stopped growing until their signal gradually disappeared at 03:00 on the next day.

5 Following the analysis mentioned above, freshly formed SOA was argued to dominantly drive the first-stage particle growth on August 6 (Fig. 3e), 12, and 15, 2014 (Fig. S5). On the other hand, newly formed SOA and NH_4NO_3 were likely the major contributors to second-stage particle growth. Again, large uncertainties in modeled concentrations may exist because of the lack of direct measurements of chemical species in nanometer particles of various sizes.

4.3 Two-stage new particle growth-B to CCN size

10 Among the three two-stage growth-B NPF events, the longest shrinkage (approximately 4 h) in grown new particles occurred on June 23, 2014 (Fig. 4a). According to our analysis, the first-stage particle growth on that day was driven by SOA because the estimated sulfuric acid and observed NO_3^- plus NH_4^+ yielded either a small percentage or negligible contribution to particle growth. The D_{pg} of newly formed particles increased from 17 nm at 11:20 to 79 nm at 17:20, with a GR of 10 nm h^{-1} . From 11:20 to 17:20, the mixing ratio of O_x increased from 74 ppb to 122 ppb (Fig. 4b). The net increase in the observed OOA was $12.2 \mu\text{g m}^{-3}$ during this period (Fig. 4c), while the required amount of SOA was estimated as $4.1 \mu\text{g m}^{-3}$. SOA was very likely to be the major contributor to particle growth in this period. As independently reported by Wu et al. (2016), the hygroscopicity parameter of 50 nm atmospheric particles decreased from ~ 0.15 to ~ 0.05 during the same event.

The D_{pg} of newly formed particles stopped growing at 79 nm from 17:20 through 18:00 and then decreased from 79 nm to 52 nm at 21:22, with a decrease rate of 8 nm h^{-1} . During this period of shrinkage, the observed mixing ratio of O_x largely decreased from 130 ppb to 80 ppb, and the observed OOA decreased from $16.2 \mu\text{g m}^{-3}$ to $11.4 \mu\text{g m}^{-3}$ (Fig. 4b, c). However, the concentrations of NH_4^+ were almost constant. Repartition of the semivolatile SOA in gas and particle phases was hypothesized to cause the evaporation of semivolatile SOA to the gas phase. The shrinkage may also be argued as being attributable to the spatial heterogeneity of NPF, but modeling of size-segregated number concentration is required to confirm this.

25 After 21:22, D_{pg} restarted to increase from ~ 50 nm to 90 nm over 4 h. The formation of NH_4NO_3 likely yielded an important contribution to the second stage of particle growth—a net observed increase of $4.5 \mu\text{g m}^{-3}$ versus the required amount of $8.4 \mu\text{g m}^{-3}$. SOA may also contribute to the second stage of particle growth according to a net increase in OOA by $1.5 \mu\text{g m}^{-3}$ (Fig. 4c). After the second stage of growth, the D_{pg} of new particles experienced small oscillations at ~ 90 nm until the signal was overwhelmed completely by aged plumes.

30 Following similar observations on June 23, reduced photochemical reaction activities were also argued to cause the shrinkage in newly formed particles on June 11 and July 26, 2014 (Fig. S6). The observed and modeled results for the two

days imply that NH_4NO_3 played an important role in new particle growth only at night. In the daytime, SOA likely acted as the major contributor.

4.4 Statistical analysis of factors related to new particle growth

The growth rate of newly formed particles is mainly determined by the concentrations of condensable vapors such as sulfuric acid, organics of various volatilities, nitric acid, and ammonia (Zhang et al., 2012; Ehn et al., 2014; Man et al., 2015; Lee et al., 2019). In contrast, D_{pgmax} values are determined by the total amount of vapors condensed on grown new particles, which may or may not have a positive correlation with the concentrations of these vapors (Zhu et al., 2019). The values of D_{pgmax} were plotted against those of GR in Fig. 5a (two variables during the first growth period were used to determine the occurrence of two-stage particle growth) and found to be widely scattered with $r=0.23$. When three circled points were excluded, D_{pgmax} was significantly correlated with GR, but the r value was still as low as 0.48 (Fig. 5a). GR alone is not sufficient to characterize the growth of newly formed particles considering their potential impacts on the climate, and both D_{pgmax} and GR should be alternatively used.

As mentioned above, SOA and NH_4NO_3 are likely two major contributors to particle growth in different periods of NPF events, with small contributions of sulfuric acid. Fig. 5b shows the net hourly increases in OOA and NH_4NO_3 against the hourly required masses for particle growth, assuming densities of $1.5 \mu\text{g m}^{-3}$ for OOA and $1.7 \mu\text{g m}^{-3}$ for NH_4NO_3 . Both OOA and NH_4NO_3 generally increase with increasing required masses and reasonably satisfy the required masses, but they are largely scattered in Fig. 5b. It remains challenging to accurately quantify the contributors to the growth of newly formed particles.

The generation of OOA and HNO_3 is strongly related to oxidation reactions during the daytime. Thus, we further plotted D_{pgmax} and GR against O_x ($\text{O}_x = \text{NO}_2 + \text{O}_3$) in the particle growth period during the daytime. Fig. 5c shows a good correlation between D_{pgmax} and O_x (hourly average value when D_{pgmax} reached) with $r=0.80$ and $P<0.01$. The values of O_x in Class I NPF events were significantly smaller than those in Class II and Class III with $P<0.05$, and the lower O_x could be one of the factors for the lack of apparent particle growth in Class I. In addition, there was no significant difference in O_x between Class II and Class III. Including O_x , other factors, such as condensational sink, should also affect the particle growth in Class I, II, and III NPF events (Guo et al., 2020). Fig. 5d shows a significant correlation between GR and $\bar{\text{O}}_x$ (average value during the entire growth period) with $r=0.67$ and $P<0.01$. The decreased r value implies that the response of GR to the increase in O_x is highly variable.

Oxidation products of biogenic VOCs, such as highly oxygenated molecules (HOMs), have been reportedly overwhelmed to determine the condensation growth of newly formed particles in the small size range because of their low volatilities (Ehn et al., 2014; Lee et al., 2019). In this study, the clear seasonal boundary of Class I and Class II + III NPF events—for example, 100% of Class I events in winter versus 7% and 93% of Class I and Class II+III events in

summer—also points toward the importance of oxidation products of biogenic VOCs in particles growing from ~10 nm to larger sizes. In the summertime, theoretically increased emissions of biogenic VOCs and enhanced photochemical reactions indicated by O_x are expected to generate more HOMs for the growth of particles from ~10 nm to larger sizes. In spring, approximately half of the NPF events are subject to Class I. However, there were no Class III events. The distinctive seasonal particle growth patterns may further imply that the amount of oxidation products of biogenic VOCs not only determines the growth of new particles from ~10 nm to larger sizes, but also the CCN size. However, direct measurements of HOMs in small-sized nanoparticles were unavailable to support this argument. In fact, such measurements remain challenging among the research community, as reviewed by Lee et al. (2019).

4.5 Final SP during Class III NPF events

The potential contribution of new particles to the population of CCN was evaluated using the calculated final SP. For Class III NPF events, the final SPs are listed in Table 1. For example, in the one-stage growth NPF event on August 25, 2014 (Fig. 2e), D_{pg} grew beyond 50 nm at 19:00. At 19:46, the integral value of new particles larger than 50 nm increased to a maximum of $1.0 \times 10^4 \text{ cm}^{-3}$. The maximum value of SP_{50} was thus estimated as the final SP, which was 42%. After 22:30, D_{pg} reached 70 nm. The integral value of grown new particles larger than 70 nm reached a maximum of $7.6 \times 10^3 \text{ cm}^{-3}$ at 24:00. The final SP_{70} was estimated to be 32%. In the two-stage new particle growth on June 27, 2014 (Fig. 3a), the number concentrations of the integrated new particles larger than 50 nm reached a maximum value of $1.1 \times 10^4 \text{ cm}^{-3}$ at 21:32. The final SP_{50} was estimated to be 73%. Using the same method, the final SP_{70} was estimated to be 49%, also at 21:32.

Overall, in Class III NPF events, the final SP_{50} varied from 42% to 85%, with a median of 70%. Meanwhile, the final SP_{70} varied from 31% to 69%, with a median of 49%. Our results imply that a significant fraction of new particles can grow to CCN size prior to being removed by atmospheric processes. Considering that high SS occasionally occurs in the atmosphere (Fan et al., 2018), new particles with D_{pg} increasing up to 50 nm may also be activated as CCN. Thus, > 40% of new particles in 11 out of 27 NPF events in the summer of 2014 can reach 50 nm and may eventually contribute to the population of CCN.

4.6 Spatial heterogeneity of NPF

The spatial heterogeneity of NPF can be clearly identified using high time-resolution measurements. Two NPF events were used as examples to demonstrate the spatial heterogeneity.

The NPF event on August 6, 2014 (Fig. 3e) clearly exhibited spatial heterogeneity; the signal of new particles largely dropped to a negligible level approximately one hour after 11:37 and then increased to a detectable level (Fig. 3e). At approximately 17:40, D_{pg} jumped from 25 nm to 50 nm within five min, indicating a large spatial heterogeneity before and after 17:40–17:50. New particles observed after 17:51 were hypothesized to experience a growth similar to the trend in the

white dashed line (Fig. 3e) in the upwind atmosphere during the period from 11:37 to 17:51.

Moreover, both the number concentrations and D_{pg} of new particles exhibited an inverted bell-shape at 23:00–01:51 on August 6, 2014 (Fig. 3e). The inverted bell-shape very likely reflects the spatial heterogeneity of NPF in the upwind atmosphere at a certain spatial range. The new particle signal was clearly enhanced after 01:51 on August 7, 2014. The new particles observed after the time were hypothesized to experience a growth similar to the trend in the white dashed line (Fig. 3e) in the upwind atmosphere.

The NPF event on June 23 also exhibited clear spatial heterogeneity (Fig. 4a). From 12:00 to 18:00, $N_{8-200nm}$ oscillated at $1.2 \pm 0.2 \times 10^4 \text{ cm}^{-3}$ (Fig. 4b). In approximately 20 min, $N_{8-200nm}$ increased to a higher level and then oscillated at $1.5 \pm 0.2 \times 10^4 \text{ cm}^{-3}$ from 18:20 on June 23 to 01:30 on June 24. $N_{8-200nm}$ then oscillated at $1.0 \pm 0.1 \times 10^4 \text{ cm}^{-3}$ from 01:50 to 04:15 on June 24.

Based on the time series of new particle number concentrations and their sizes observed, the spatial heterogeneity of NPF can be inferred to have occurred universally in each NPF event. This phenomenon should be considered for accurately evaluating the climate impacts of NPF events.

5 Conclusions

In this study, we investigated 46 NPF events in Beijing's urban atmosphere through three campaigns, with particular attention to the growth behaviors of newly formed particles. First, we found seasonal variations in the maximum sizes of newly grown particles. For instance, D_{pgmax} was found to exceed 75 nm in 11 out of 27 NPF events in summer. However, no apparent growth in new particles with $D_{pgmax} < 20 \text{ nm}$ was observed in December across all events, which could be attributed to several factors, such as the lower level of O_x and high condensation sink. Correlation analyses also suggest that the concentrations of O_x may play an important role in determining D_{pgmax} . This finding may allow us to rethink the seasonal impacts of NPF events on the climate in Beijing and other urban areas in northern China.

According to the observed mixing ratio of SO_2 , sulfuric acid vapor generally yielded minor contributions to the growth of new particles. The observed and modeled concentrations of particulate chemical species suggested that the growth of newly formed particles during the daytime was mainly caused by OOA (or SOA). At night and late afternoon, the increased amount of NH_4NO_3 can reasonably support new particle growth in most Class III NPF events. Secondary organics were also an important contributor to nighttime new particle growth in most Class III NPF events. Nevertheless, direct measurements of secondary organics in nanometer particles of different sizes are required to confirm their contribution.

To verify the climate impacts of NPF events, the final SP_{50} and final SP_{70} need to be quantified. In Class III NPF events, the final SP_{50} and final SP_{70} varied from 42% to 85% and from 31% to 69%, respectively, implying that a significant fraction of new particles can grow to CCN size. Our observations also indicated that each NPF event exhibited spatial heterogeneity to some extent, which may be attributable to varying photochemical reaction activities. When photochemical reaction

activities are low, the growth of new particles may reach an upper limit or even decline. These factors should also be considered for accurately evaluating the climate impacts of NPF events in the future.

Data availability. The research data can be accessed upon contact with the corresponding author (Xiaohong Yao (xhyao@ouc.edu.cn) and Yujiao Zhu (zhuyujiao@sdu.edu.cn)).

Author contributions. XY designed the research. YZ, MZ and YS conducted the field measurements. LH and XL run the CMAQ model. LM and YZ analyzed the data and wrote the paper. YG, YS, HG and XY helped to interpretation of the results. XY revised the original manuscript. All authors contributed toward improving the paper.

Competing interests. The authors declare that they have no conflict of interest.

10 Acknowledgment

This research was supported by the National Key Research and Development Program in China (grant no. 2016YFC0200504), the Natural Science Foundation of China (grant no. 41576118 and grant no. 41430646).

References

15 Asmi, E., Kivekäs, N., Kerminen, V.M., Komppula, M., Hyvärinen, A.P., Hatakka, J., Viisanen, Y., and Lihavainen, H.: Secondary new particle formation in Northern Finland Pallas site between the years 2000 and 2010, *Atmos. Chem. Phys.*, 11, 12959-12972, doi: 10.5194/acp-11-12959-2011, 2011.

Baek, J., Hu, Y.T., Odman, M.T., and Russell, A.G.: Modeling secondary organic aerosol in CMAQ using multigenerational oxidation of semi-volatile organic compounds, *J. Geophys. Res.*, 116, D22204, doi: 10.1029/2011JD015911, 2011.

20 Brean, J., Harrison, Roy., Shi, Z., Beddows, D. C. S., Acton, W., Nicholas Hewitt, C., Squires, F. A., and Lee J.: Observations of highly oxidized molecules and particle nucleation in the atmosphere of Beijing, *Atmos. Chem. Phys.*, 19, 14933–14947, doi: 10.5194/acp-19-14933-2019, 2019.

Burkart, J., Hodshire, A. L., Mungall, E. L., Pierce, J. R., Collins, D.B., Ladino, L. A., Lee, A. K., Irish, V., Wentzell, J. J., Liggio, J., and Papakyriakou, T.: Organic condensation and particle growth to CCN sizes in the summertime marine Arctic is driven by materials more semivolatile than at continental sites, *Geophys. Res. Lett.*, 44, 10725–10734, doi: 10.1002/2017GL075671, 2017.

25 Byun, D and Schere, K.L.: Review of the Governing Equations, Computational Algorithms, and Other Components of the Models-3 Community Multiscale Air Quality (CMAQ) Modeling System. *Applied Mechanics Reviews*. 59, 51-77, doi: 10.1115/1.2128636, 2006.

- Carlton, A.G., Bhave, P.V., Napelenok, S.L., Edney, E.O., Sarwar, G., Pinder, R.W., Pouliot, G.A., and Houyoux, M.: Model Representation of Secondary Organic Aerosol in CMAQv4.7, *Environ. Sci. Technol.*, 44, 8553-8560, doi: 10.1021/es100636q, 2010.
- 5 **Chen, X., Yang, W., Wang, Z., Li, J., Hu, M., An, J., Wu, Q., Wang, Z., Chen, H., Wei, Y., Du, H., and Wang, D.: Improving new particle formation simulation by coupling a volatility-basis set (VBS) organic aerosol module in NAQPMS+APM, *Atmos. Environ.*, 204, 1–11, doi: 10.1016/j.atmosenv.2019.01.053, 2019.**
- Chu, B., Kerminen, V., Bianchi, F., Yan, C., Petäjä, T., and Kulmala, M.: Atmospheric new particle formation in China, *Atmos. Chem. Phys.*, 19, 115-138, doi: 10.5194/acp-19-115-2019, 2019.
- Dal Maso, M., Kulmala, M., Riipinen, I., Wagner, R., Hussein, T., Aalto, P.P., Lehtinen, K.E.J.: Formation and growth of fresh atmospheric aerosols: eight years of aerosol size distribution data from SMEAR II, Hyytiälä, Finland. *Boreal Env.* 10 *Res.*, 10, 323-336, doi: <http://www.borenav.net/BER/pdfs/ber10/ber10-323.pdf>, 2005.
- Du, W., Zhao, J., Wang, Y., Zhang, Y., Wang, Q., Xu, W., Chen, C., Han, T., Zhang, F., Li, Z., Fu, P., Li, J., Wang, Z., and Sun, Y.: Simultaneous measurements of particle number size distributions at ground level and 260 m on a meteorological tower in urban Beijing, China, *Atmos. Chem. Phys.*, 17, 6797–6811, doi: 10.5194/acp-17-6797-2017,** 15 **2017.**
- Ehn, M., Thornton, J.A., Kleist, E., Sipilä, M., Junninen, H., Pullinen, I., Springer, M., Rubach, F., Tillmann, R., Lee, B., Lopez-Hilfiker, F., Andres, S., Acir, I., Rissanen, M., Jokinen, T., Schobesberger, S., Kangasluoma, J., Kontkanen, J., Nieminen, T., Kurtén, T., Nielsen, L.B., Jørgensen, S., Kjaergaard, H.G., Canagaratna, M., Maso, M.D., Berndt, T., Petäjä, T., Wahner, A., Kerminen, V., Kulmala, M., Worsnop, D.R., Wildt, J., and Mentel, T.F.: A large source of low-volatility secondary organic aerosol, *Nature*, 506, 476-479, doi: 10.1038/nature13032, 2014.
- Fan, J., Rosenfeld, D., Zhang, Y., Giangrande, S.E., Li, Z., Machado, L.A.T., Martin, S.T., Yang, Y., Wang, J., Artaxo, P., Barbosa, H.M.J., Braga, R.C., Comstock, J.M., Feng, Z., Gao, W., Gomes, H.B., Mei, F., Pöhlker, C., Pöhlker, M.L., Pöschl, U., Souza, R.A.F.: Substantial convection and precipitation enhancements by ultrafine aerosol particles, *Science*, 359, 411-418. doi: <http://science.sciencemag.org/>, 2018.
- 25 Gordon, H., Kirkby, J., Baltensperger, U., Bianchi, F., Breitenlechner, M., Curtius, J., Dias, A., Dommen, J., Donahue, N.M., Dunne, E.M., Duplissy, J., Ehrhart, S., Flagan, R.C., Frege, C., Fuchs, C., Hansel, A., Hoyle, C.R., Kulmala, M., Kürten, A., Lehtipalo, K., Makhmutov, V., Molteni, U., Rissanen, M.P., Stozhkov, Y., Tröstl, J., Tsagkogeorgas, G., Wagner, R., Williamson, C., Wimmer, D., Winkler, P.M., Yan, C., and Carslaw, K.S.: Causes and importance of new particle formation in the present-day and preindustrial atmospheres, *J. Geophys. Res. Atmos.*, 122, 8739-8760, doi: 30 10.1002/2017JD026844, 2017.
- Guenther, A., Karl, T., Harley, P., Wiedinmyer, C., Palmer, P.I., Geron, C.: Estimates of global terrestrial isoprene emissions

using MEGAN (Model of Emissions of Gases and Aerosols from Nature), *Atmos. Chem. Phys.*, 6, 3181-3210, doi: <https://hal.archives-ouvertes.fr/hal-00295995>, 2006.

- Guo, S., Hu, M., Zamora, M. L., Peng, J., Shang, D., Zheng, J., Du, Z., Wu, Z., Shao, M., Zeng, L., Molina, M. J., and Zhang, R.: Elucidating severe urban haze formation in China, *P. Natl. Acad. Sci. USA*, 111, 17373–17378, doi: 10.1073/pnas.1419604111, 2014.
- Guo, S., Hu, M., Peng, J., Wu, Z., Zamora, M. L., Shang, D., Du, Z., Zheng, J., Fang, X., Tang, R., Wu, Y., Zeng, L., Shuai, S., Zhang, W., Wang, Y., Ji, Y., Zhang, A., Wang, W., Zhang, F., Zhao, J., Gong, X., Wang, C., Molina, M., and Zhang, R.: Remarkable nucleation and growth of ultrafine particles from vehicular exhaust. *P. Natl. Acad. Sci.*, 117(7), 3427-3432, doi: 10.1073/pnas.1916366117, 2020.
- Hayes, P.L., Carlton, A.G., Baker, K.R., Ahmadov, R., Washenfelder, R.A., Alvarez, S., Rappenglück, B., Gilman, J.B., Kuster, W.C., de Gouw, J.A., Zotter, P., Prévôt, A.S.H., Szidat, S., Kleindienst, T.E., Offenberg, J.H., Ma, P.K., and Jimenez, J.L.: Modeling the formation and aging of secondary organic aerosols in Los Angeles during CalNex 2010, *Atmos. Chem. Phys.*, 15, 5773-5801, doi: 10.5194/acp-15-5773-2015, 2015.
- He, K.B., Yang, F.M., Ma, Y.L., Zhang, Q., Yao, X.H., Chan, C.K., Cadle, S., Chan, T., and Mulawa, P.: The characteristics of PM_{2.5} in Beijing, China. *Atmos. Environ.*, 35, 4959-4970, doi: 10.1016/S1352-2310(01)00301-6, 2001.
- Huang, W., Saathoff, H., Shen, X., Ramisetty, R., Leisner, T., and Mohr, C.: Chemical Characterization of Highly Functionalized Organonitrates Contributing to Night-Time Organic Aerosol Mass Loadings and Particle Growth, *Environ. Sci. Technol.*, 53, 1165-1174, doi: 10.1021/acs.est.8b05826, 2019.
- Kanawade, V. P., Tripathi, S. N., Chakraborty, A., and Yu, H.: Chemical Characterization of Sub-micron Aerosols during New Particle Formation in an Urban Atmosphere, *Aerosol Air Qual. Res.*, 20(6): 1294-1305, doi: 10.4209/aaqr.2019.04.0196, 2020.
- Kerminen, V., Chen, X., Vakkari, V., Petäjä, T., Kulmala, M., and Bianchi, F.: Atmospheric new particle formation and growth: review of field observations, *Environ. Res. Lett.*, 13, 103003, doi: 10.1088/1748-9326/aadf3c, 2018.
- Kuang, C., McMurry, P.H., and McCormick, A.V.: Determination of cloud condensation nuclei production from measured new particle formation events, *Geophys. Res. Lett.*, 36, L09822, doi: 10.1029/2009GL037584, 2009.
- Kulmala, M., Dal Maso, M., Mäkelä, J. M., Pirjola, L., Väkevä, M., Aalto P., Miiikkulainen, P., Hämeri, K., O'dowd, C.D.: On the formation, growth and composition of nucleation mode particles, *Tellus*, 53B, 479–490, doi: 10.1034/j.1600-0889.2001.530411.x, 2001.
- Kulmala, M., Vehkamäki, H., Petäjä, T., Dal Maso, M., Lauri, A., Kerminen, V.M., Birmili, W., and McMurry, P.H.: Formation and growth rates of ultrafine atmospheric particles: a review of observations, *J. Aerosol Sci.*, 35, 143-176, doi: 10.1016/j.jaerosci.2003.10.003, 2004.

- Kulmala, M., and Kerminen, V.: On the formation and growth of atmospheric nanoparticles, *Atmos. Res.*, 90, 132-150, doi: 10.1016/j.atmosres.2008.01.005, 2008.
- Kulmala, M., Petäjä, T., Nieminen, T., Sipilä, M., Manninen, H. E., Lehtipalo, K., Dao Maso, M., Aalto, P. P., Junninen, H., Paasonen, P., Riipinen, I., Lehtinen, K. E. J., Laaksonen, A., and Kerminen, V-M.: Measurement of the nucleation of atmospheric aerosol particles, *Nat. Protoc.*, 7, 1651–1667, doi: org/10.1038/nprot.2012.091, 2012.
- Kulmala, M., Petäjä, T., Kerminen, V-M., Kujansuu, J., Ruuskanen, T., Ding, A., Nie, W., Hu, M., Wang, Z., Wu, Z., Wang, L., and Worsnop, D. R.: On secondary new particle formation in China, *Front. Environ. Sci. Eng.*, 10 (5): 8, doi:10.1007/s11783-016-0850-1, 2016.
- Knote C., Hodzic A., Jimenez J.L., Volkamer R., Orlando J.J., Baidar S., Brioude J., Fast J., Gentner D.R., Goldstein A.H., Hayes P.L., Knighton W.B., Oetjen H., Setyan A., Stark H., Thalman R., Tyndall G., Washenfelder R., Waxman E. and Zhang Q.: Simulation of semi-explicit mechanisms of SOA formation from glyoxal in aerosol in a 3-D model, *Atmos. Chem. Phys.*, 14, 6213-6239, doi:10.5194/acp-14-6213-2014, 2014.
- Laakso, L., Merikanto, J., Vakkari, V., Laakso, H., Kulmala, M., Molefe, M., Kgabi, N., Mabaso, D., Carslaw, K.S., Spracklen, D.V., Lee, L.A., Reddington, C.L., and Kerminen, V.M.: Boundary layer nucleation as a source of new CCN in savannah environment, *Atmos. Chem. Phys.*, 13, 1957-1972, doi: 10.5194/acp-13-1957-2013, 2013.
- Lee, B.H., Mohr, C., Lopez-Hilfiker, F.D., Lutz, A., Hallquist, M., Lee, L., Romer, P., Cohen, R.C., Iyer, S., Kurtén, T., Hu, W., Day, D.A., Campuzano-Jost, P., Jimenez, J.L., Xu, L., Ng, N.L., Guo, H., Weber, R.J., Wild, R.J., Brown, S.S., Koss, A., de Gouw, J., Olson, K., Goldstein, A.H., Seco, R., Kim, S., McAvey, K., Shepson, P.B., Starn, T., Baumann, K., Edgerton, E.S., Liu, J., Shilling, J.E., Miller, D.O., Brune, W., Schobesberger, S., D'Ambro, E.L., and Thornton, J.A.: Highly functionalized organic nitrates in the southeast United States: Contribution to secondary organic aerosol and reactive nitrogen budgets, *P. Natl. Acad. Sci. USA.*, 113, 1516-1521, doi: 10.1073/pnas.1508108113, 2016.
- Lee, S., Gordon, H., Yu, H., Lehtipalo, K., Haley, R., Li, Y., and Zhang, R.: New Particle Formation in the Atmosphere: From Molecular Clusters to Global Climate, *J. Geophys. Res. Atmos.*, 124, 7098-7146, doi: 10.1029/2018JD029356, 2019.
- Levy, M.E., Zhang, R., Khalizov, A.F., Zheng, J., Collins, D.R., Glen, C.R., Wang, Y., Yu, X., Luke, W., Jayne, J.T., and Olaguer, E.: Measurements of submicron aerosols in Houston, Texas during the 2009 SHARP field campaign, *J. Geophys. Res. Atmos.*, 118, 10, 518-10, 534, doi: 10.1002/jgrd.50785, 2013.
- Li, J., Yin, Y., Li, P., Li, Z., Li, R., Cribb, M., Dong, Z., Zhang, F., Li, J., Ren, G., Jin, L., and Li, Y.: Aircraft measurements of the vertical distribution and activation property of aerosol particles over the Loess Plateau in China, *Atmos. Res.*, 155, 73-86, doi: 10.1016/j.atmosres.2014.12.004, 2015.
- Liu, X., Zhang, Y., Cheng, S., Xing, J., Zhang, Q., Streets, D.G., Jang, C., Wang, W., and Hao, J.: Understanding of regional

air pollution over China using CMAQ, part I performance evaluation and seasonal variation, *Atmos. Environ.*, 44, 2415-2426, doi: 10.1016/j.atmosenv.2010.03.035, 2010.

Liu, X., Zhang, Y., Xing, J., Zhang, Q., Wang, K., Streets, D.G., Jang, C., Wang, W., and Hao, J.: Understanding of regional air pollution over China using CMAQ, part II. Process analysis and sensitivity of ozone and particulate matter to precursor emissions, *Atmos. Environ.*, 44, 3719-3727, doi: 10.1016/j.atmosenv.2010.03.036, 2010.

Liu, X.H., Zhu, Y.J., Zheng, M., Gao, H.W., and Yao, X.H.: Production and growth of new particles during two cruise campaigns in the marginal seas of China, *Atmos. Chem. Phys.*, 14, 7941-7951, doi: 10.5194/acp-14-7941-2014, 2014.

Lu, Y., Yan, C., Fu, Y., Chen, Y., Liu, Y., Yang, G., Wang, Y., Bianchi, F., Chu, B., Zhou, Y., Yin, R., Baalbaki, R., Garmash, O., Deng, C., Wang, W., Liu, Y., Petäjä, T., Kerminen, V., Jiang, J., Kulmala, M., and Wang, L.: A proxy for atmospheric daytime gaseous sulfuric acid concentration in urban Beijing, *Atmos. Chem. Phys.*, 19, 1971-1983, doi: 10.5194/acp-19-1971-2019, 2019.

Ma, N., Zhao, C., Tao, J., Wu, Z., Kecorius, S., Wang, Z., Größ, J., Liu, H., Bian, Y., Kuang, Y., Teich, M., Spindler, G., Müller, K., van Pinxteren, D., Herrmann, H., Hu, M., and Wiedensohler, A.: Variation of CCN activity during new particle formation events in the North China Plain, *Atmos. Chem. Phys.*, 16, 8593-8607, doi: 10.5194/acp-16-8593-2016, 2016.

Man, H., Zhu, Y., Ji, F., Yao, X., Lau, N.T., Li, Y., Lee, B.P., and Chan, C.K.: Comparison of Daytime and Nighttime New Particle Growth at the HKUST Supersite in Hong Kong, *Environ. Sci. Technol.*, 49, 7170-7178, doi: 10.1021/acs.est.5b02143, 2015.

Matsui, H., Koike, M., Kondo, Y., Takegawa, N., Wiedensohler, A., Fast, J.D., Zaveri, R. A.: Impact of new particle formation on the concentrations of aerosols and cloud condensation nuclei around beijing, *J. Geophys. Res. Atmos.*, 116, D19208, doi: 10.1029/2011JD016025, 2011.

Nieminen, T., Lehtinen, K. E. J., and Kulmala, M.: Sub-10 nm particle growth by vapor condensation – effects of vapor molecule size and particle thermal speed, *Atmos. Chem. Phys.*, 10, 9773–9779, doi: 10.5194/acp-10-9773-2010, 2010.

Petäjä, T., Mauldin, R.L., Kosciuch, E., McGrath, J., Nieminen, T., Paasonen, P., Boy, M., Adamov, A., Kotiaho, T., Kulmala, M.: Sulfuric acid and OH concentrations in a boreal forest site, *Atmos. Chem. Phys.*, 9, 7435–7448, doi: www.atmos-chem-phys.net/9/7435/2009/, 2009.

Qi, J., Liu, X., Yao, X., Zhang, R., Chen, X., Lin, X., Gao, H., and Liu, R.: The concentration, source and deposition flux of ammonium and nitrate in atmospheric particles during dust events at a coastal site in northern China, *Atmos. Chem. Phys.*, 18, 571-586, doi: 10.5194/acp-18-571-2018, 2018.

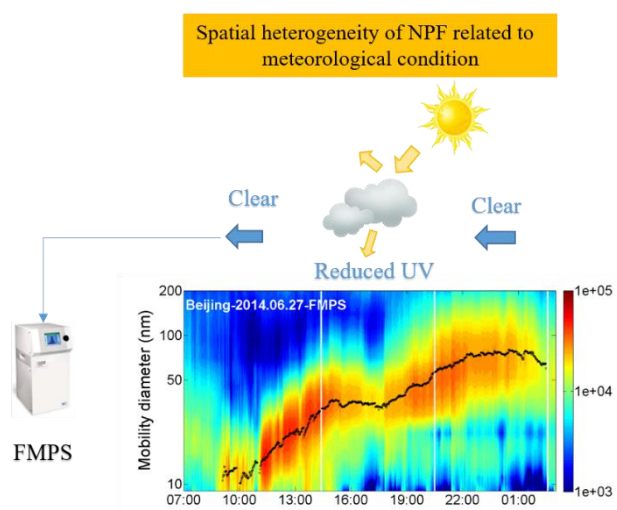
Quan, J., Liu, Y., Liu, Q., Jia, X., Li, X., Gao, Y., Ding, D., Li, J., and Wang, Z.: Anthropogenic pollution elevates the peak height of new particle formation from planetary boundary layer to lower free troposphere, *Geophys. Res. Lett.*, 44,

- Riipinen, I., Pierce, J. R., Yli-Juuti, T., Nieminen, T., Häkkinen, S., Ehn, M., Junninen, H., Lehtipalo, K., Petäjä, T., Slowik, J., Chang, R., Shantz, N. C., Abbatt, J., Leaitch, W. R., Kerminen, V.-M., Worsnop, D. R., Pandis, S. N., Donahue, N. M., and Kulmala, M.: Organic condensation: a vital link connecting aerosol formation to cloud condensation nuclei (CCN) concentrations, *Atmos. Chem. Phys.*, 11, 3865–3878, doi: 10.5194/acp-11-3865-2011, 2011.
- Rodelas, R. R., Chakraborty, A., Perdrix, E., Tison, E., and Riffault, V.: Real-time assessment of wintertime organic aerosol characteristics and sources at a suburban site in northern France, *Atmos. Environ.*, 203, 48-61, doi: 10.1016/j.atmosenv.2019.01.035 2019.
- Rose, C., Sellegri, K., Moreno, I., Velarde, F., Ramonet, M., Weinhold, K., Krejci, R., Andrade, M., Wiedensohler, A., Ginot, P., and Laj, P.: CCN production by new particle formation in the free troposphere, *Atmos. Chem. Phys.*, 17, 1529-1541, doi: 10.5194/acp-17-1529-2017, 2017.
- Sabaliauskas, K., Jeong, C., Yao, X., Jun, Y., Jadidian, P., and Evans, G.J.: Five-year roadside measurements of ultrafine particles in a major Canadian city, *Atmos. Environ.*, 49, 245-256, doi: 10.1016/j.atmosenv.2011.11.052, 2012.
- Seinfeld, J. I.: From Air Pollution to Climate Change, *Environment: Science and Policy for Sustainable Development*, 15, *Atmos. Chem. Phys.*, 40:7, 26-26, doi: 10.1080/00139157.1999.10544295, 1998.
- Vu, T.V., Delgado-Saborit, J.M., and Harrison, R.M.: A review of hygroscopic growth factors of submicron aerosols from different sources and its implication for calculation of lung deposition efficiency of ambient aerosols, *Air Qual. Atmos. Health.*, 8, 429-440, doi: 10.1007/s11869-015-0365-0, 2015.
- Wang, M., Kong, W., Marten, R., He, X., Chen, D., Pfeifer, J., Heitto, A., Kontkanen, J., Dada, L., Kürten, A., Yli-Juuti, T., Manninen, H., Amanatidis, S., Amorim, A., Baalbaki, R., Baccarini, A., Bell, D., Bertozzi, B., Bräkling, S., Brilke, S., Murillo, U. C., Chiu, R., Chu, B., De Menezes, L-P., Duplissy, J., Finkenzeller, H., Carracedo, L. G., Granzin, M., Guida, R., Hansel, A., Hofbauer, V., Krechmer, J., Lehtipalo, K., Lamkaddam, H., Lampimäki, M., Lee, C.P., Makhmutov, V., Marie, G., Mathot, S., Mauldin, R. L., Mentler, B., Müller, T., Onnela, A., Partoll, E., Petäjä, T., Philippov, M., Pospisilova, V., Ranjithkumar, A., Rissanen, M., Rörup, B., Scholz, W., Shen, J., Simon, M., Sipilä, M., Steiner, G., Stolzenburg, D., Tham, Y. J., Tomé, A., Wagner, A. C., Wang, D. S., Wang, Y., Weber, S.K., Winkler, P. M., Wlasits, P. J., Wu, Y., Xiao, M., Ye, Q., Zauner-Wieczorek, M., Zhou, X., Volkamer, R., Riipinen, I., Dommen, J., Curtius, J., Baltensperger, U., Kulmala, M., Worsnop, D. R., Kirkby, J., Seinfeld, J. H., El-Haddad, I., Flagan, R. C., and Donahue, N. M.: Rapid growth of new atmospheric particles by nitric acid and ammonia condensation, *Nature* 581, 184–189, doi: 10.1038/s41586-020-2270-4, 2020.
- Wang, Z.B., Hu, M., Sun, J., Yue, D., Shen, X., Zhang, Y., Pei, X., Cheng, Y., and Wiedensohler, A.: Characteristics of regional new particle formation in urban and regional background environments in the North China Plain, *Atmos. Chem. Phys.*, 13, 10159–10170, doi: 10.5194/acp-13-10159-2013, 2013.

- Wang, Z.B., Hu, M., Pei, X.Y., Zhang, R.Y., Paasonen, P., Zheng, J., Yue, D.L., Wu, Z.J., Boy, M., and Wiedensohler, A.: Connection of organics to atmospheric new particle formation and growth at an urban site of Beijing, *Atmos. Environ.*, 103, 7-17, doi:10.1016/j.atmosenv.2014.11.069, 2015.
- 5 Wehner, B., Wiedensohler, A., Tuch, T. M., Wu, Z. J., Hu, M., Slanina, J., and Kiang, C. S.: Variability of the aerosol number size distribution in Beijing, China: New particle formation, dust storms, and high continental background, *Geophys. Res. Lett.*, 31, L22108, doi: 10.1029/2004GL021596, 2004.
- Whitby, K. T.: The physical characteristics of sulfur aerosols, *Atmos. Environ.*, 12(1-3), 135-159, <https://doi.org/10.1016/B978-0-08-022932-4.50018-5>, 1978.
- Wiedensohler, A., Cheng, Y.F., Nowak, A., Wehner, B., Achtert, P., Berghof, M., Birmili, W., Wu Z.J., Hu, M., Zhu, T.,
10 Takegawa, N., Kita, K., Kondo, Y., Lou, S.R., Hofzumahaus, A., Holland, F., Wahner, A., Gunthe, S.S, Rose, D., Su, H., Pöschl, U.: Rapid aerosol particle growth and increase of cloud condensation nucleus activity by secondary aerosol formation and condensation: A case study for regional air pollution in northeastern china, *J. Geophys. Res.*, 114, D00G08, doi: org/10.1029/2008JD010884, 2009.
- Wu, Z., Hu, M., Liu, S., Wehner, B., Bauer, S., Maßling, A., Wiedensohler, A., Petäjä, T., Dal Maso, M., and Kulmala, M.:
15 New particle formation in Beijing, China: Statistical analysis of a 1-year data set, *J. Geophys. Res.*, 112, doi: 10.1029/2006JD007406, 2007.
- Wu, Z.J., Zheng, J., Shang, D.J., Du, Z.F., Wu, Y.S., Zeng, L.M., Wiedensohler, A., and Hu, M.: Particle hygroscopicity and its link to chemical composition in the urban atmosphere of Beijing, China, during summertime, *Atmos. Chem. Phys.*, 16, 1123-1138, doi: 10.5194/acp-16-1123-2016, 2016.
- 20 Xu, W.Q., Han, T.T., Du, W., Wang, Q.Q., Chen, C., Zhang, Y.J., Li, J., Fu, P.Q., Wang, Z.F., Worsnop, D.R., Sun, Y.L.: Effects of aqueous-phase and photochemical processing on secondary organic aerosol formation and evolution in Beijing, China, *Environ. Sci. Technol.*, 51, 762-770, doi: 10.1021/acs.est.6b04498, 2017.
- Yao, X., Choi, M.Y., Lau, N.T., Lau, A.P.S., Chan, C.K., and Fang, M.: Growth and Shrinkage of New Particles in the Atmosphere in Hong Kong, *Aerosol Sci. Tech.*, 44, 639-650, doi: 10.1080/02786826.2010.482576, 2010.
- 25 Yao, X., Lau, N.T., Fang, M., and Chan, C.K.: Real-Time Observation of the Transformation of Ultrafine Atmospheric Particle Modes, *Aerosol Sci. Tech.*, 39, 831-841, doi: 10.1080/02786820500295248, 2005.
- Yu, F., Luo, G.: Simulation of particle size distribution with a global aerosol model: contribution of nucleation to aerosol and CCN number concentrations, *Atmos. Chem. Phys.*, 9, 7691-7710, doi: www.atmos-chem-phys.net/9/7691/2009/, 2009.
- Yu, F., and Hallar, A.G.: Difference in particle formation at a mountaintop location during spring and summer: Implications
30 for the role of sulfuric acid and organics in nucleation, *J. Geophys. Res. Atmos.*, 119, 12,246-12,255, doi: 10.1002/2014JD022136, 2014.

- Yu, H., Ortega, J., Smith, J.N., Guenther, A.B., Kanawade, V.P., You, Y., Liu, Y., Hosman, K., Karl, T., Seco, R., Geron, C., Pallardy, S.G., Gu, L., Mikkilä, J., Lee, S.H.: New Particle Formation and Growth in an Isoprene-Dominated Ozark Forest: From Sub-5 nm to CCN-Active Sizes, *Aerosol Sci. Technol.*, 48, 1285-1298, doi: www.tandfonline.com/loi/uast20, 2014.
- 5 Yu, H., Ren, L., Huang, X., Xie, M., He, J., and Xiao, H.: Iodine speciation and size distribution in ambient aerosols at a coastal new particle formation hotspot in China, *Atmos. Chem. Phys.*, 19, 4025-4039, doi: 10.5194/acp-19-4025-2019, 2019.
- 10 Yue, D.L., Hu, M., Zhang, R.Y., Wang, Z.B., Zheng, J., Wu, Z.J., Wiedensohler, A., He, L.Y., Huang, X.F., Zhu, T. The roles of sulfuric acid in new particle formation and growth in the mega-city of Beijing. *Atmos. Chem. Phys.*, 10(10), 4953-4960, doi:10.5194/acp-10-4953-2010, 2010.
- Yue, D.L., Hu, M., Zhang, R.Y., Wu, Z.J., Su, H., Wang, Z.B., Peng, J., He, L., Huang, X., Gong, Y., Wiedensohler, A. Potential contribution of new particle formation to cloud condensation nuclei in Beijing, *Atmos. Environ.*, 45, 6070-6077, doi: 10.1016/j.atmosenv.2011.07.037, 2011.
- Zhang, Q., Xue, D., Liu, X.H., Gong, X., Gao, H.W.: Process analysis of PM_{2.5} pollution events in a coastal city of China using CMAQ, *J. Environ. Sci. (China)*, 79, 225-238, doi: www.tandfonline.com/loi/uast20, 2019.
- 15 Zhang, R., Khalizov, A., Wang, L., Hu, M., and Xu, W.: Nucleation and Growth of Nanoparticles in the Atmosphere, *Chem. Rev.*, 112, 1957-2011, doi: 10.1021/cr2001756, 2012.
- Zhang, R., Wang, G., Guo, S., Zamora, M.L., Ying, Q., Lin, Y., Wang, W., Hu, M., and Wang, Y.: Formation of Urban Fine Particulate Matter, *Chem. Rev.*, 115, 3803-3855, doi: 10.1021/acs.chemrev.5b00067, 2015.
- 20 Zhang, Y. M., Zhang, X. Y., Sun, J. Y., Hu, G. Y., Shen, X. J., Wang, Y. Q., Wang, T. T., Wang, D. Z., and Zhao, Y.: Chemical composition and mass size distribution of PM₁ at an elevated site in central east China, *Atmos. Chem. Phys.*, 14, 12237-12249, doi: 10.5194/acp-14-12237-2014, 2014.
- Zhu, Y., Li, K., Shen, Y., Gao, Y., Liu, X., Yu, Y., Gao, H., and Yao, X.: New particle formation in the marine atmosphere during seven cruise campaigns, *Atmos. Chem. Phys.*, 19, 89-113, doi: 10.5194/acp-19-89-2019, 2019.
- 25 Zhu, Y., Sabaliauskas, K., Liu, X., Meng, H., Gao, H., Jeong, C., Evans, G.J., and Yao, X.: Comparative analysis of new particle formation events in less and severely polluted urban atmosphere, *Atmos. Environ.*, 98, 655-664, doi: 10.1016/j.atmosenv.2014.09.043, 2014.
- Zhu, Y., Yan, C., Zhang, R., Wang, Z., Zheng, M., Gao, H., Gao, Y., and Yao, X.: Simultaneous measurements of new particle formation at 1 s time resolution at a street site and a rooftop site, *Atmos. Chem. Phys.*, 17, 9469-9484, doi: 10.5194/acp-17-9469-2017, 2017.
- 30 Zimmerman, N., Jeong, C., Wang, J.M., Ramos, M., Wallace, J.S., and Evans, G.J.: A source-independent empirical

correction procedure for the fast mobility and engine exhaust particle sizes, *Atmos. Environ.*, 100, 178-184, doi:
10.1016/j.atmosenv.2014.10.054, 2015.



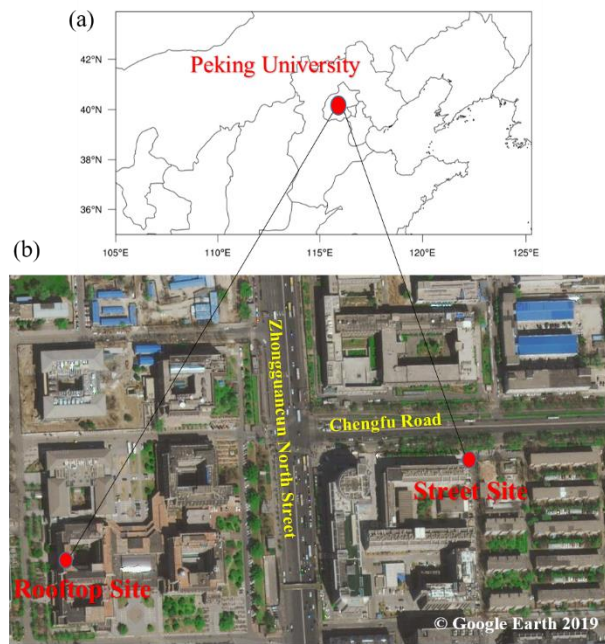


Fig. 1 Locations of sampling sites (a) and satellite imagery of the two sampling sites (b) (downloaded from <https://www.earthol.com/>).

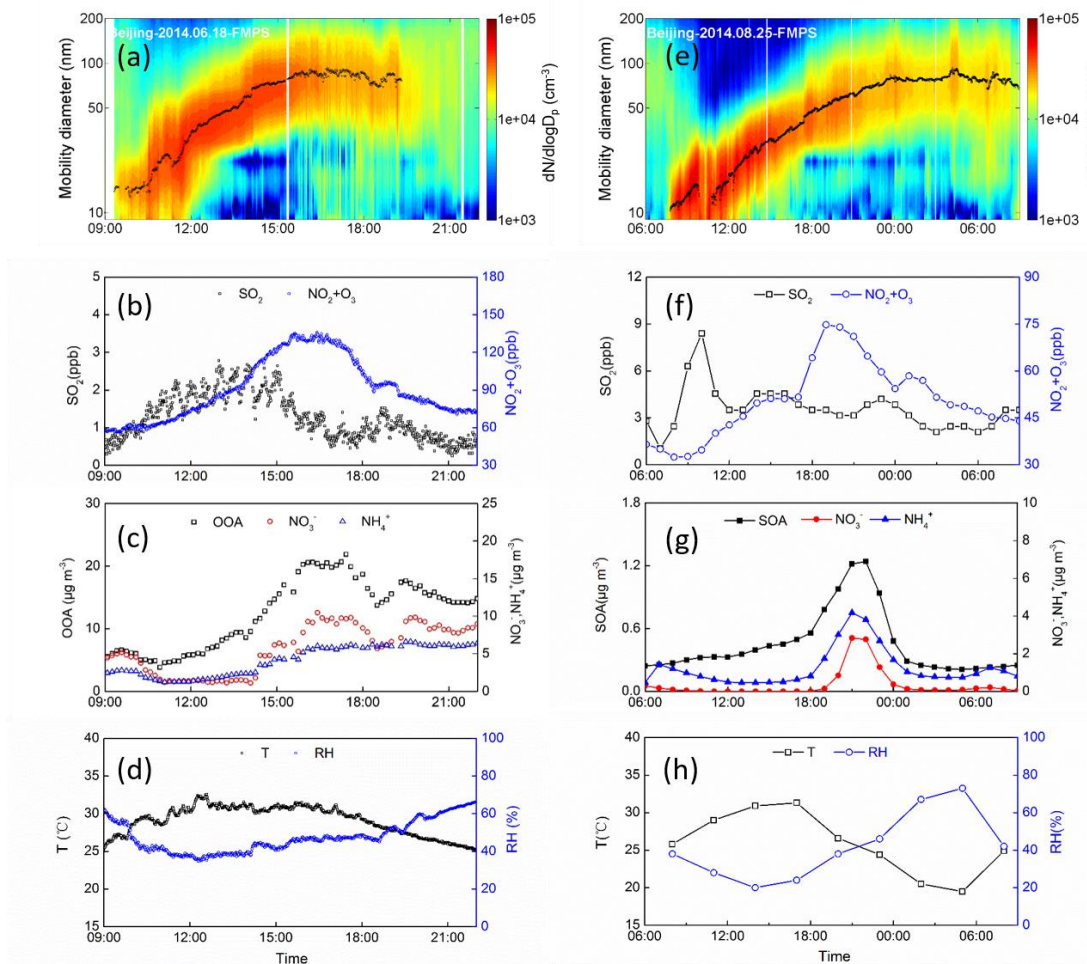


Fig. 2 NPF events on June 18 and August 25, 2014 ((a, e) contour plot of particle number concentration; (b, f) time series of observed mixing ratios of SO₂ and NO₂+O₃; (c) time series of observed **OOA**, NO₃⁻ and NH₄⁺ in PM_{1.0}; (d, h) time series of ambient T and RH; (g) time series of modeled SOA, NO₃⁻ and NH₄⁺ in PM_{2.5}).

5

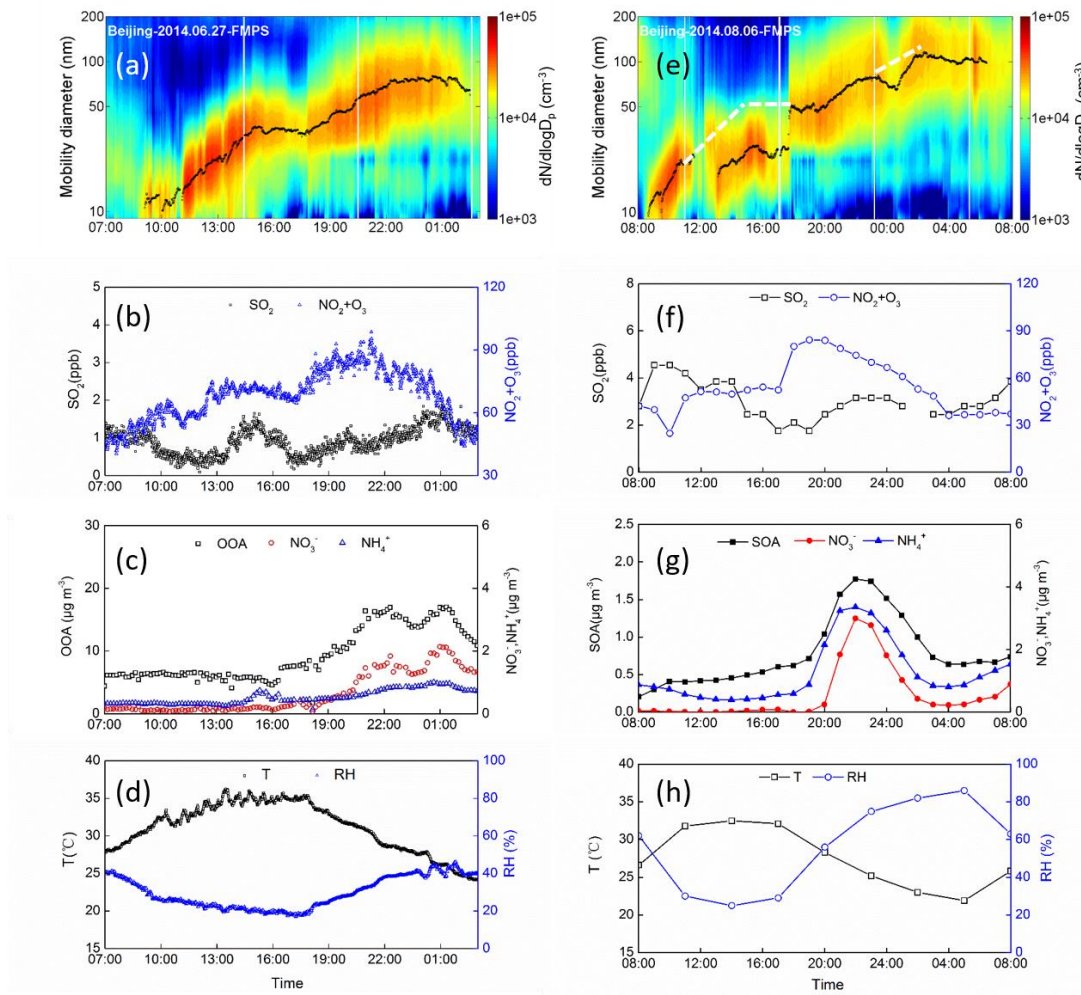


Fig. 3 NPF events on June 27 and August 6, 2014 ((a, e) contour plot of particle number concentration; (b, f) time series of observed mixing ratios of SO_2 and NO_2+O_3 ; (c) time series of observed **OOA**, NO_3^- and NH_4^+ in $\text{PM}_{1.0}$; (d, h) time series of ambient T and RH (g) time series of modeled SOA, NO_3^- and NH_4^+ in $\text{PM}_{2.5}$).

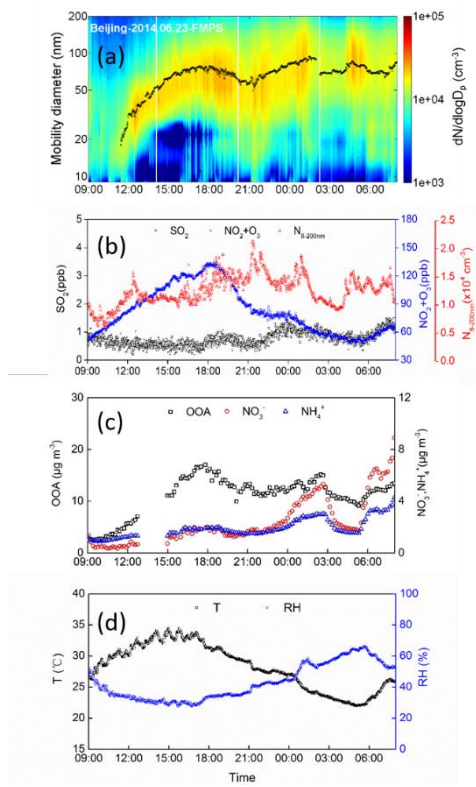
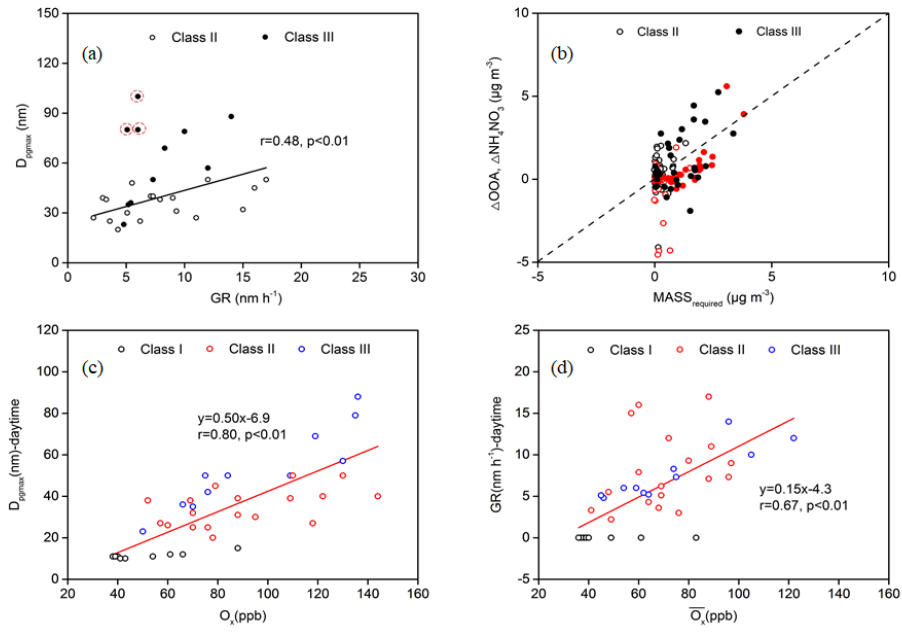


Fig. 4 NPF event on June 23, 2014 ((a) contour plot of particle number concentration; (b) time series of observed mixing ratios of SO₂, NO₂+O₃, and N_{8-200nm}; (c) time series of observed **OOA**, NO₃⁻ and NH₄⁺ in PM_{1.0}; (d) time series of ambient T and RH).



5 **Fig. 5** Relationship between D_{pgmax} and GR (a); hourly variations in measured **OOA** (black mark) and NH_4NO_3 (red mark, assuming NO_3^- to be completely associated with NH_4^+) versus required masses of **OOA** and NH_4NO_3 for corresponding particle growth (b); relationship between D_{pgmax} in the daytime and the corresponding maximum O_x (c), and relationship between GRs in the daytime and the average mixing ratio of O_x (d).

Table1 Characteristics of NPF events in Beijing

Season	Date	Period	GR or SR (nm h ⁻¹)	NMINP (10 ⁴ #cm ⁻³)	D _{pgmax} (nm)	SO ₂ (ppb) ^d	SP (%)	O ₃ +NO ₂ (ppb) ^e
Winter	10 Dec 2011*	9:00-15:00	-	1.5	11	2.5~4.4	-	36~38
	11 Dec 2011*	11:00-14:00	-	2.5	11	7.2~16	-	34~40
	14 Dec 2011*	10:00-16:00	-	1.1	11	3.1~5.8	-	31~39
	15 Dec 2011*	10:30-17:30	-	1.0	11	1.6~5.3	-	33~39
	21 Dec 2011	13:00-18:00	-	0.5	10	1.4~3.5	-	33~43
	21 Dec 2011*	9:00-12:00	-	1.1	12	2.5~5.9	-	22~61
	22 Dec 2011	10:00-15:00	-	1.3	10	2.3~6.0	-	32~41
	22 Dec 2011*	11:30-15:40	-	2.3	10	2.3~7.6	-	23~41
	23 Dec 2011	11:00-14:00	-	0.7	10	3.5~16	-	32~43
	23 Dec 2011*	9:40-16:30	-	0.7	10	3.6~9.2	-	38~41
Spring	12 Apr 2012	9:20-18:20	2.2	2.9	27	1.0~2.3	-	41~57
	13 Apr 2012	11:20-19:00	6.2	1.5	25	1.4~3.6	-	61~76
	14 Apr 2012	12:00-19:00	9.3	0.8	31	2.0~7.7	-	73~88
	15 Apr 2012	11:30-19:00	-	1.7	12	0.0~2.1	-	57~66
	16 Apr 2012	10:22-14:20	7.9	1.2	38	1.3~3.7	-	52~69
	25 Apr 2012	10:07-20:00	-	1.0	11	0.0~1.9	-	47~54
	25 Apr 2012*	10:07-20:00	-	1.1	11	0.0~1.9	-	47~54
	27 Apr 2012	9:40-16:00	-	2.1	15	-	-	-
	27 Apr 2012*	9:40-16:00	-	1.4	15	-	-	-
Summer	1 Jun 2014	12:00-16:00	-	1.1	15	0.4~1.5	-	77~88
	3 Jun 2014	8:00-12:00	4.3	3.0	20	1.2~10	-	56~78
	4 Jun 2014	11:30-22:00	11	1.2	27	1.2~3.7	-	67~118
	7 Jun 2014	9:00-(+1) 3:00	5.5	1.3	48	0.0~1.3	-	32~64
	8 Jun 2014	9:00-14:00	12	1.5	50	3.5~9.0	-	41~110
	9 Jun 2014	10:55-19:40	7.1	1.1	40	1.0~4.5	-	55~122
	11 Jun 2014	9:20-(+1) 3:20	5.4/5.1 ^a /9.0 ^b	1.1	36/84 ^c	0.0~1.2	82/57 ^e	43~89
	12 Jun 2014	8:00-15:00	3.6	3.1	25	1.2~7.3	-	50~87
	18 Jun 2014	9:20-20:20	14	1.8	88	0.4~2.8	78/50 ^e	56~136
	23 Jun 2014	11:20-(+1) 1:22	10/8.0 ^a /10 ^b	0.5	79/90 ^c	0.2~1.3	N/A ^f	53~135
	27 Jun 2014	9:00-(+1) 3:00	5.2/9.7 ^b	1.5	35/75 ^c	0.1~1.9	73/49 ^e	44~99
	28 Jun 2014	7:00-19:00	3.0	1.8	39	0.6~10	-	15~106
	29 Jun 2014	8:50-15:00	7.3	0.7	40	1.7~9.2	-	62~144
	8 Jul 2014	9:30-21:00	16	1.0	45	0.9~4.3	-	52~79
	9 Jul 2014	10:00-17:30	15	2.4	32	0.9~4.3	-	42~91
	12 Jul 2014	9:00-(+1) 4:00	6.0	1.6	80	1.8~3.5	66/43 ^e	36~84
	13 Jul 2014	7:30-(+1) 4:00	6.0	2.5	100	2.1~5.6	56/31 ^e	37~78
	14 Jul 2014	8:00-20:00	17	2.5	50	3.2~5.3	-	41~135
	25 Jul 2014	11:20-22:00	9.0	0.6	39	3.9~6.0	-	86~109
	26 Jul 2014	14:33-(+1) 8:00	12/8.2 ^a /7.5 ^b	0.9	57/120 ^c	5.3~11	85/69 ^e	23~130
6 Aug 2014	8:41-(+1) 8:00	4.8/10 ^b	1.4	23/115 ^c	1.4~4.6	70/63 ^e	25~82	
12 Aug 2014	10:00-22:00	7.3/6.5 ^b	1.3	50/75 ^c	2.1~4.6	N/A ^f	47~109	
15 Aug 2014	10:10-(+1) 3:42	8.3/8.7 ^b	0.9	69/110 ^c	2.1~6.3	N/A ^f	41~119	

	24 Aug 2014	8:00-19:00	3.3	3.0	38	3.9~8.1	-	30~52
Summer	25 Aug 2014	7:50-(+1) 9:00	5.1	2.4	80	2.1~8.4	42/32 ^e	32~75
	26 Aug 2014	9:00-23:00	5.1	1.1	30	0.7~7.0	-	44~95
	27 Aug 2014	12:25-14:30	-	1.1	12	-	-	-

*: The NPF events occurred on the street site.

^a: Refers to the shrinkage rates of two-stage growth-B.

^b: Refers to the second-stage growth rates.

5 ^c: Refers to the D_{pgmax} of the second-stage growth.

^d: Refers to the mixing ratio range of SO_2 during the NPF period.

^e: Refers to the **SP** with the D_{pg} increasing up to 50 nm and 70 nm, respectively.

^f: Refers to Equation 5 not applicable for calculating SP during the NPF events.

^g: Refers to the mixing ratio range of O_x (NO_2+O_3) during the NPF period.

10